Electronic Supplementary Information

Modulation of Circularly Polarized Luminescence Through Excited-State Symmetry Breaking and Interbranched Exciton Coupling in Helical Push-Pull Organic Systems

Kais Dhbaibi,[a,h] Ludovic Favereau,[a,*] Monika Srebro-Hooper,[b,*] Cassandre Quinton,[a] Nicolas Vanthuyne,[c] Lorenzo Arrico,[d] Thierry Roisnel,[a] Bassem Jamoussi,[e] Cyril Poriel,[a] Clément Cabanetos,[f] Jochen Autschbach,[g] and Jeanne Crassous[a,*]

a. Univ Rennes, CNRS, ISCR-UMR 6226, ScanMAT–UMS 2001, F-35000 Rennes, France. E-mails: jeanne.crassous@univ-rennes1.fr; ludovic.favereau@univ-rennes1.fr

b. Faculty of Chemistry, Jagiellonian University, Gronostajowa 2, 30-387 Krakow, Poland. E-mail: srebro@chemia.uj.edu.pl

c. Aix Marseille University, CNRS, Centrale Marseille, iSm2, Marseille, France

d. Dipartimento di Chimica e Chimica Industriale (University of Pisa), via Moruzzi 13, 56124, Pisa, Italy

e. Departement of Environmental Sciences, Faculty of Meteorology, Environment and Arid Land Agriculture, King Abdulaziz university, 21589 Jeddah, Saudi Arabia

f. MOLTECH-Anjou, CNRS UMR 6200, University of Angers, 2 Bd Lavoisier, 49045 Angers, France

g. Department of Chemistry, University at Buffalo, State University of New York, Buffalo, NY 14260, USA

h. University of Gabès, Faculty of Science of Gabès, Zrig, 6072 Gabès, Tunisia

Table of Contents

A. General methods

^{1}H and ^{13}C NMR spectra were recorded at room temperature on a Bruker Avance III 300 or 400 or a Bruker Avance I 500 at Centre Régional de Mesures Physiques de l'Ouest (CRMPO), Université de Rennes 1. Chemical shifts δ are given in ppm, relative to an internal standard of residual deuterated solvent ($CDCl_3$: δ = 7.26 ppm for ^{1}H NMR, δ = 77.16 ppm for ^{13}C NMR; CD_2Cl_2: δ = 5.32 ppm for ^{1}H NMR, δ = 53.84 ppm for ^{13}C NMR), and coupling constants *J* are given in Hz.

High-resolution mass spectra (HR-MS) determinations were performed at CRMPO on a Bruker MaXis 4G and Ultraflex III by ASAP (+ or -) or ESI techniques with CH_2Cl_2 as solvent. Experimental and calculated masses are given with consideration of the mass of the electron.

UV-visible (UV-vis, in M^{-1} cm^{-1}) absorption spectra were recorded on a UV-2401PC Shimadzu spectrophotometer. Fluorescence spectra and lifetimes τ were measured on an FL 920 Edimburgh fluorimeter, while absolute fluorescence quantum yields Φ were recorded with a Hamamatsu C9920–03 integrating sphere.

Specific rotations (in deg cm^2 g^{-1}) were measured in a 1.0 dm thermostated quartz cell on a PerkinElmer Model 341 polarimeter. Electronic circular dichroism spectra (ECD, in M^{-1} cm^{-1}) were recorded on a Jasco J-815 Circular Dichroism Spectrometer (IFR140 facility - Biosit - Université de Rennes 1). Molar rotations are given in deg cm^2 $dmol^{-1}$.

Circularly polarized luminescence (CPL) measurements were performed using an in-house-developed CPL spectrofluoropolarimeter (see Reference 1 for details on the instrument). The samples were excited using a 90°-geometry with a green InGaN (3 mm, 2 V) LED source (Luckylight Electronics Co., LTD, λ_{max} = 517 nm, HWHM = 15 nm). The following parameters were used: emission slit width ≈ 10 nm, integration time = 4 sec, scan speed = 60 nm/min, accumulations = 4. The concentration of all the samples was 10^{-6} M.

Electrochemical measurements were performed with a potentiostat-galvanostat AutoLab PGSTAT 302N controlled by resident General Purpose Electrochemical System (GPES 4.9) software using a conventional single-compartment three-electrode cell. The working and auxiliary electrodes were platinum electrodes and the reference electrode was the saturated potassium chloride calomel electrode (SCE). The supporting electrolyte was 0.2 M Bu_4NPF_6 in CH_2Cl_2 and solutions were purged with argon before the measurements. The scan rate was 200 mV/s. All potentials are given relative to SCE.

Thin-layer chromatography (TLC) was performed on aluminum sheets precoated with Merck 5735 Kieselgel 60F254. Column chromatography was carried out with Merck 5735 Kieselgel 60F (0.040-0.063 mm mesh).

Chemicals were purchased from Sigma-Aldrich, Alfa Aesar or TCI Europe, and used as received.

[1] F. Zinna, T. Bruhn, C. A. Guido, J. Ahrens, M. Bröring, L. Di Bari, G. Pescitelli, *Chem. Eur. J.* **2016**, *22*, 16089-16098.

B. Synthetic procedures

Rac-, *M*-, and *P*-2,15-bis(trimethylsilyl-ethynyl)[6]helicene (*rac*-, *M*-, and *P*-**H6(TMS)$_2$**),[2] and 6-bromo-2-hexyl-1*H*-benzoisoquinoline-1,3(2*H*)-dione (**NPhBr**)[3] were prepared using previously reported procedures. *P*- and *M*-**2** have been recently reported by us.[4]

Synthetic procedure for *P*- and *M*-**1** and *P*- and *M*-**2** (only the procedure for the *P* enantiomers is described):

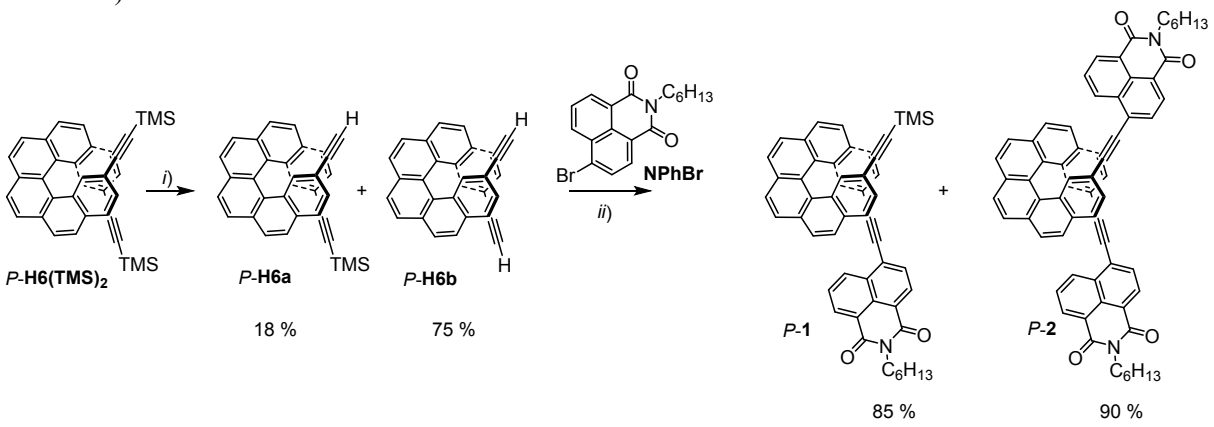

Scheme S1. Synthesis of enantiopure helicene-naphthalimide derivatives *P*-**1** and *P*-**2**. TMS: trimethylsilyl. Reaction conditions: *i*) TBAF, $CHCl_3$, r.t.; *ii*) $Pd(PPh_3)_4$, CuI, Et_3N/toluene, 50°C, **NPhBr**. Yield: 85 % (**1**) and 90 % (**2**). For clarity reasons, only the *P* stereochemistry is presented.

Enantiopure *P*-**H6(TMS)$_2$** (150 mg, 0.29 mmol) was dissolved in $CHCl_3$ (5 mL). Tetra-*n*-butylammonium fluoride (TBAF, 1.0 M solution in THF) was added dropwise to the stirred solution until full conversion of *P*-**H6(TMS)$_2$** into a mixture of partially and fully deprotected hexahelicene derivatives, *P*-**H6a** and *P*-**H6b**, respectively, occurred (the progress of the reaction was carefully monitored by TLC after the addition of each 3 drops of TBAF solution). Then, the crude reaction mixture was immediately passed through a short plug of silica gel (CH_2Cl_2) to provide a mixture of partially deprotected *P*-**H6a** (23 mg, 18 %, determinate by NMR) and fully deprotected *P*-**H6b** (81 mg, 75 %, determinate by NMR) as yellow solids, which were directly used as a statistical mixture in the next step without further purification.

The mixture of *P*-**H6a** and *P*-**H6b** and 6-bromo-2-hexyl-1*H*-benzoisoquinoline-1,3(2*H*)-dione **NPhBr** (365 mg, 0.70 mmol) were placed in an oven-dried flask of 25 mL under argon. Then 6.5 mL of dry toluene and 1.5 mL of dry Et_3N were added and the resulting solution was freed from oxygen by bubbling argon for 1 hour. $Pd(PPh_3)_4$ (30 mg, 0.03 mmol) and CuI (10 mg, 0.05 mmol) were added and the solution was refluxed for 3 hours. After cooling down to room temperature, the solution was passed through a short silica plug (CH_2Cl_2). The crude mixture was further purified by column chromatography on silica (8/2 to 5/5 for heptane/CH_2Cl_2 eluent system) to yield *P*-**1** (31 mg, 85 %) and *P*-**2** (181 mg, 90 %) as yellow solids.

P- and *M*-**1**

[2] E. Anger, M. Srebro, N. Vanthuyne, L. Toupet, S. Rigaut, C. Roussel, J. Autschbach, J. Crassous, R. Réau, *J. Am. Chem. Soc.* **2012**, *134*, 15628-15631.
[3] J. Zhengneng, L. Najun, W. Chuanfeng, J. Huajiang, L. Jianmei, Z. Qizhong, *Dyes Pigm.* **2013**, *96*, 204-210.
[4] P. Josse, L. Favereau, C. Shen, S. Dabos-Seignon, P. Blanchard, C. Cabanetos, J. Crassous, *Chem. Eur. J.* **2017**, *23*, 6277-6281.

^{1}H NMR (300 MHz, CD_2Cl_2) δ 8.68 (dd, *J* = 7.3, 1.2 Hz, 1H), 8.51 (d, *J* = 7.6 Hz, 1H), 8.32 (dd, *J* = 8.4, 1.2 Hz, 1H), 8.18 – 8.07 (m, 6H), 8.04 – 7.91 (m, 5H), 7.82 – 7.72 (m, 3H), 7.57 (dd, *J* = 8.2, 1.6 Hz, 1H), 7.29 (dd, *J* = 8.2, 1.6 Hz, 1H), 4.14 (t, *J* = 7.6 Hz, 2H), 1.70 (q, *J* = 7.3 Hz, 2H), 1.51 – 1.30 (m, 6H), 1.00 – 0.87 (m, 3H), 0.23 – 0.14 (s, 9H).

^{13}C NMR (126 MHz, CD_2Cl_2) δ 164.4, 164.1, 134.1, 133.2, 132.9, 132.7, 132.6, 132.6, 132.3, 132.1, 131.8, 131.0, 130.6, 129.7, 129.5, 128.9, 128.6, 128.5, 128.4, 128.3, 128.0, 128.0, 127.9, 127.6, 124.4, 123.7, 122.7, 120.0, 118.8, 105.5, 99.9, 94.2, 86.2, 41.0, 32.2, 30.3, 28.6, 27.4, 23.2, 14.4, 1.4, 0.1.

HR-MS Bruker Ultraflex III, MALDI; ion $[M]^{+\cdot}$, $C_{51}\,H_{41}\,N\,O_2\,Si$, m/z calculated: 727.29011, m/z experimental: 727.287 (Δ = 4 ppm).

Experimental optical rotation values

P-(+)-**1**: $[\alpha]_D^{23}$ = +2980 (± 5 %), $[\phi]_D^{23}$ = +21690 (CH_2Cl_2, 2.1·10^{-4} mol L^{-1}).

M-(-)-**1**: $[\alpha]_D^{23}$ = -2870 (± 5 %), $[\phi]_D^{23}$ = -20890 (CH_2Cl_2, 2.1·10^{-4} mol L^{-1}).

P- and *M*-**2**

^{1}H NMR (400 MHz, $CDCl_3$) δ 8.52 (dd, *J* = 7.3 Hz, 1.1 Hz, 2H), 8.36 (d, *J* = 7.5 Hz, 2H), 8.09 – 8.02 (m, 4H), 7.98 (d, *J* = 8.2 Hz, 4H), 7.82 (d, *J* = 8.6 Hz, 2H), 7.74 (bs, 2H), 7.70 (d, *J* = 7.9 Hz, 2H), 7.60 (d, *J* = 8.2 Hz, 2H), 7.55 (d, *J* = 7.6 Hz, 2H), 7.28 (dd, *J* = 8.2, 1.6 Hz, 2H), 4.14 (t, *J* = 7.5 Hz, 4H), 1.79 – 1.67 (m, 4H), 1.49 – 1.28 (m, 12H), 0.9 (t, *J* = 6.9 Hz, 6H).

^{13}C NMR (126 MHz, $CDCl_3$) δ 163.9, 163.6, 133.6, 132.5, 132.1, 132.0, 131.9, 131.3, 131.3, 130.4, 130.2, 129.0, 128.0, 128.0, 127.9, 127.6, 127.4, 127.3, 127.1, 127.0, 123.7, 122.9, 121.8, 118.4, 99.5, 85.8, 40.7, 31.7, 28.2, 26.9, 22.7, 14.2.

HR-MS Bruker MaXis 4G, ASAP (+), 370 °C; ion $[M+H]^+$, $C_{66}\,H_{51}\,N_2\,O_4$, m/z calculated: 935.38433, m/z experimental: 935.3838 (Δ = 1 ppm).

Experimental optical rotation values

P-(+)-**2**: $[\alpha]_D^{23}$ = +7530 (± 5 %), $[\phi]_D^{23}$ = +70400 (CH_2Cl_2, 2.1·10^{-4} mol L^{-1}).

M-(-)-**2**: $[\alpha]_D^{23}$ = -7380 (± 5 %), $[\phi]_D^{23}$ = -69000 (CH_2Cl_2, 2.1·10^{-4} mol L^{-1}).

C. NMR spectra

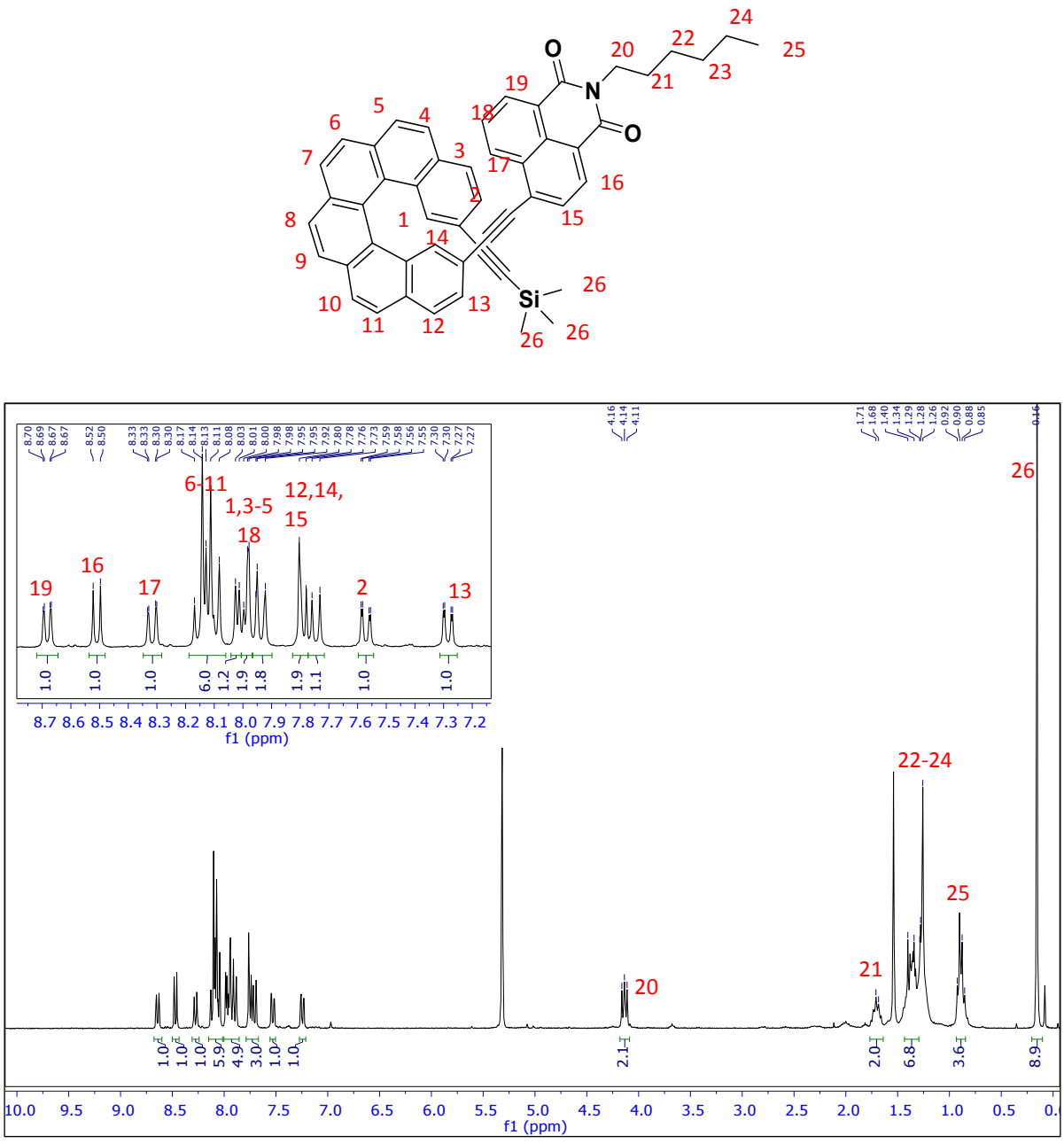

Figure S1. ^{1}H NMR spectrum of **1** in CD_2Cl_2 at 298 K (300 MHz).

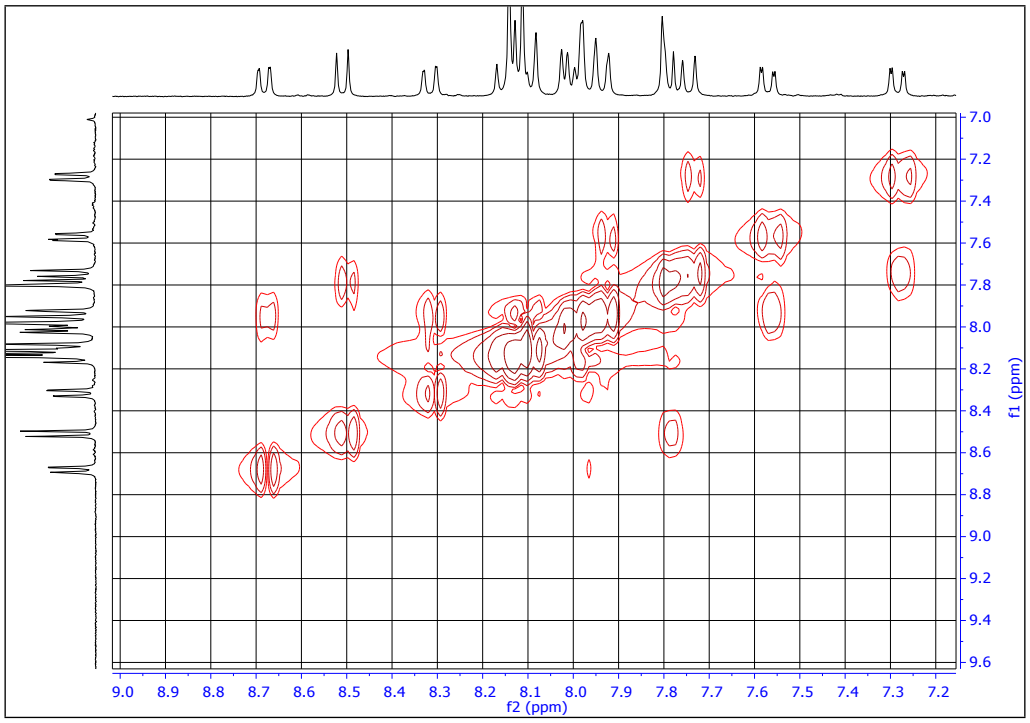

Figure S2. Region of the ^{1}H NMR COSY spectrum of **1** corresponding to the aromatic protons (300 MHz, CD_2Cl_2, 298 K).

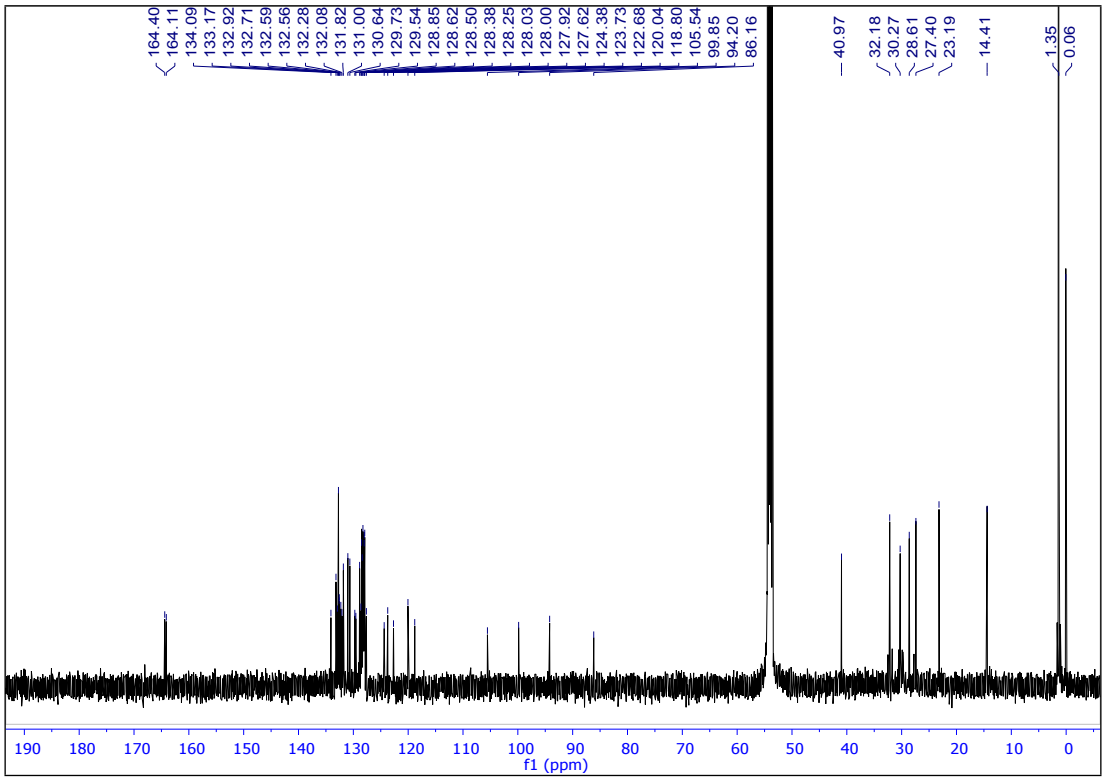

Figure S3. ^{13}C NMR spectrum of **1** in CD_2Cl_2 at 298 K (126 MHz).

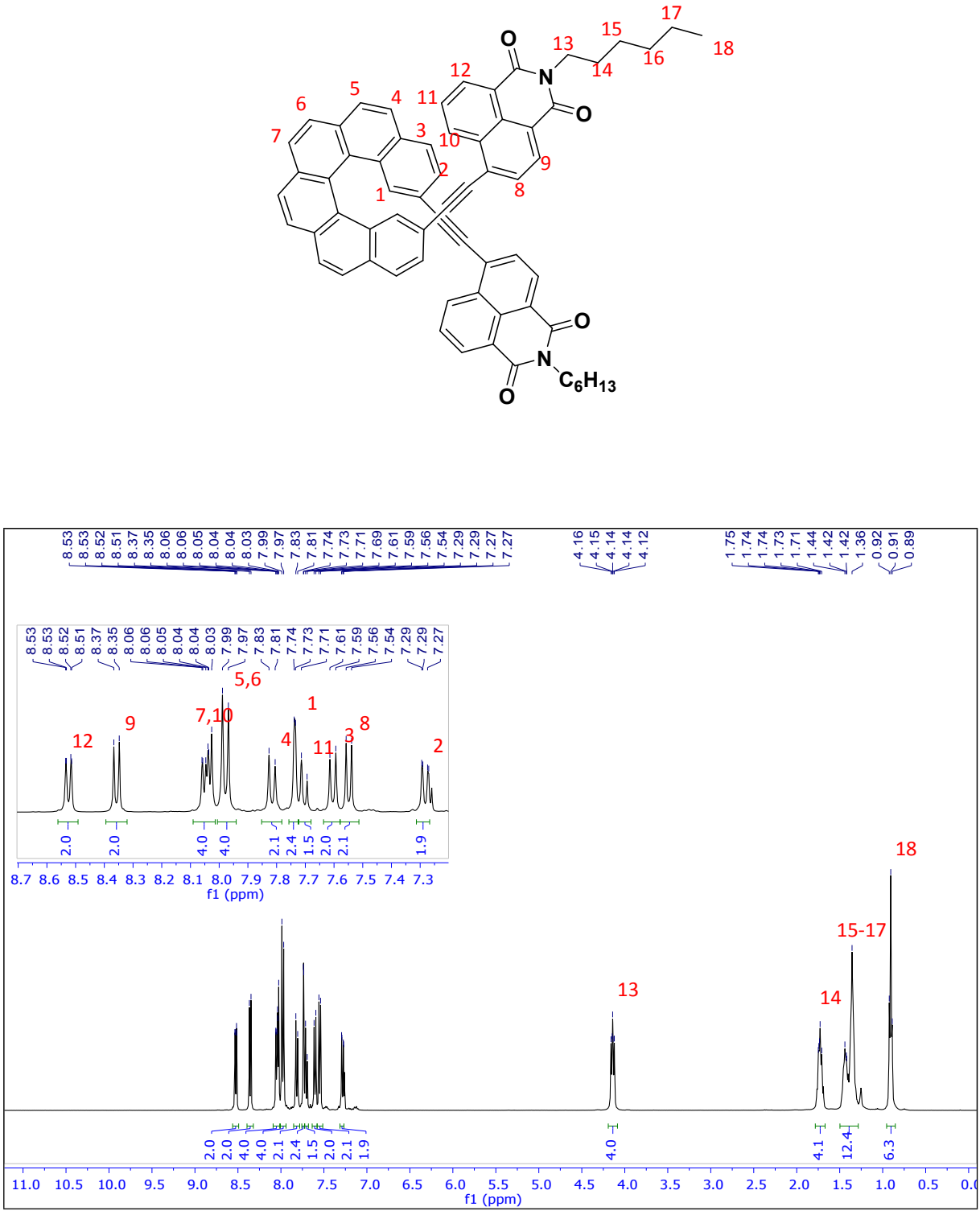

Figure S4. ^{1}H NMR spectrum of **2** in $CDCl_3$ at 298 K (400 MHz).

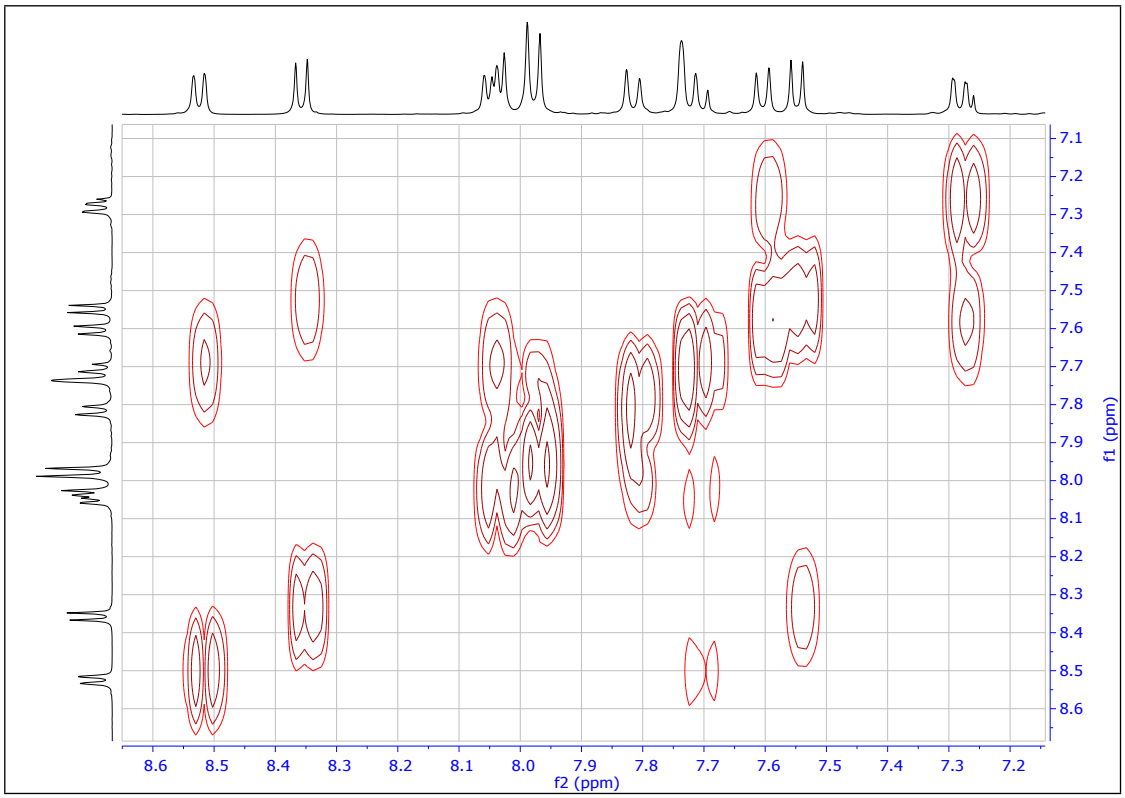

Figure S5. Region of the ^{1}H NMR COSY spectrum of **2** corresponding to the aromatic protons (400 MHz, $CDCl_3$, 298 K).

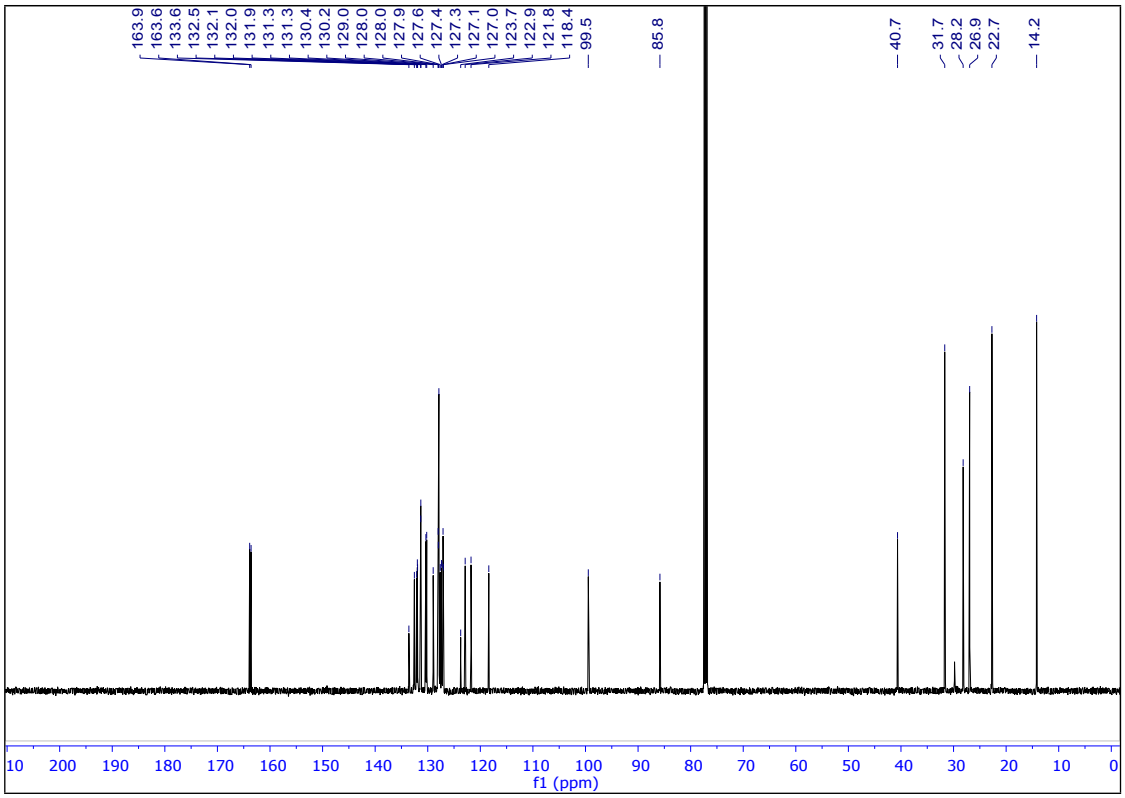

Figure S6. ^{13}C NMR spectrum of **2** in $CDCl_3$ at 298 K (126 MHz).

D. Crystal structure of 2

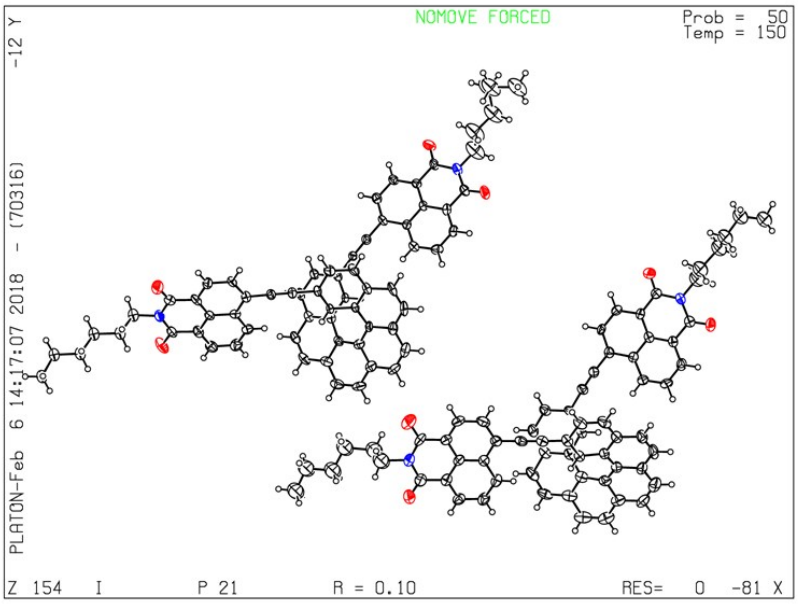

ORTEP diagram of compound **2** with ellipsoids at 50 % probability.

Table S1. X-ray crystallographic data for compound **2**.

Empirical formula	C66 H50 N2 O4
CCDC number	1894823
Formula weight (g mol^{-1})	935.08
Temperature (K)	150
Wavelength (Å)	0.71073
Crystal system	monoclinic
Space group	P 21
a (Å)	15.2114(17)
b (Å)	15.0318(19)
c (Å)	22.042(2)
α(°)	90
β(°)	93.831(4)
γ(°)	90
Volume (Å^3)	5028.7(10)
Z	4
$\rho_{calculated}$ (g cm^{-3})	1.235
Absorption coefficient (mm^{-1})	0.076
F(000)	1968
Crystal size (mm)	0.420 x 0.300 x 0.190
Crystal color	yellow
θ range for data collection (º)	3.004 to 27.484
Limiting indices	-19≤h≤19
	-19≤k≤19
	-28≤l≤28
Reflections unique	59114 / 22426 [R(int) = 0.0622]
Reflections collected [I>2s(I)]	15796
Completeness to θ_max	0.991
Absorption correction type	multi-scan
Max. and min. transmission	0.986 and 0.732
Refinement method	Full-matrix least-squares on *F*2
Data / restraints / parameters	22426 / 1 / 1177
Goodness-of-fit on *F*2	1.018
Final R indices [$I>2\sigma(I)$]	R1 = 0.0984, wR2 = 0.2509
R indices (all data)	R1 = 0.1354, wR2 = 0.2780
Largest diff. peak and hole (e Å^{-3})	1.196 and -0.804

E. Steady-state photophysical characterizations

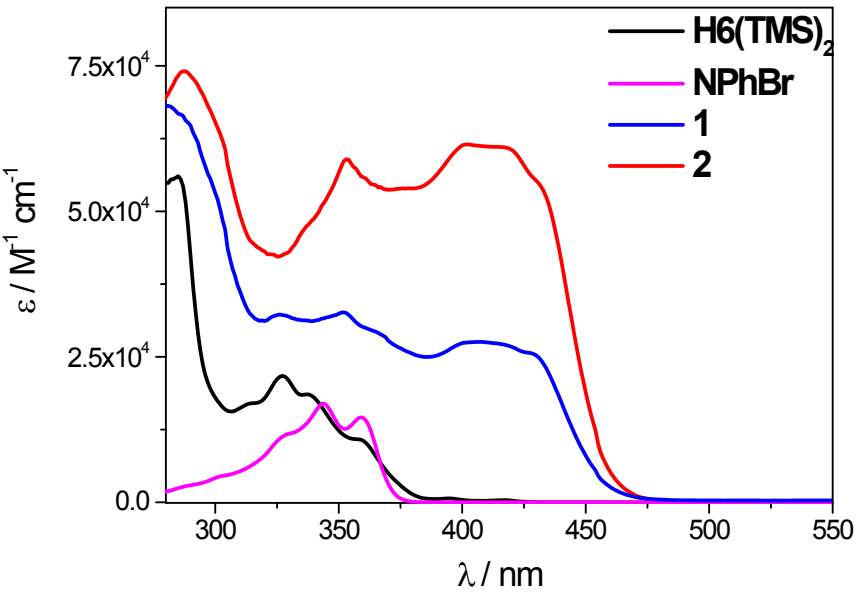

Figure S7. UV-vis spectra of **NPhBr** (pink), **H6(TMS)$_2$** (black), **1** (blue), and **2** (red) in dichloromethane solution (~10^{-6} M) at 298 K.

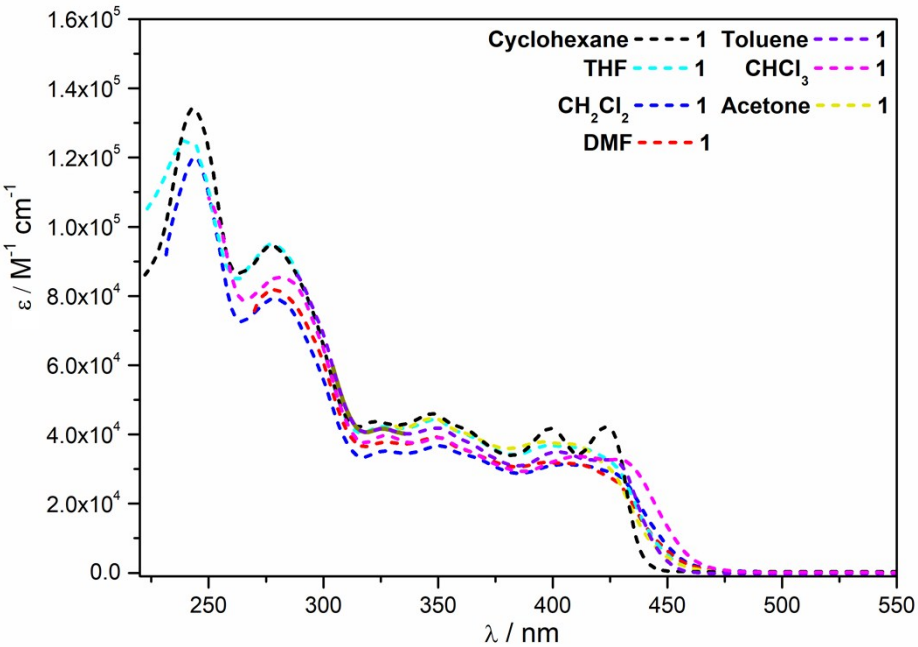

Figure S8. UV-vis spectra of **1** in cyclohexane (black), toluene (purple), THF (sky blue), $CHCl_3$ (pink), CH_2Cl_2 (blue), acetone (yellow), and DMF (red) solutions (~10^{-6} M) at 298 K.

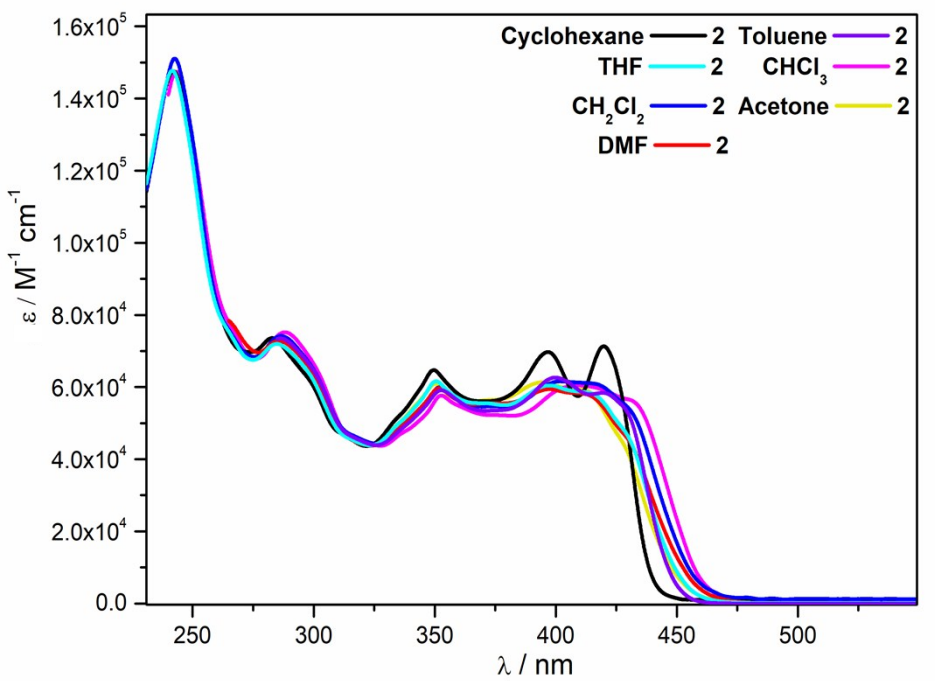

Figure S9. UV-vis spectra of **2** in cyclohexane (black), toluene (purple), THF (sky blue), $CHCl_3$ (pink), CH_2Cl_2 (blue), acetone (yellow), and DMF (red) solutions (~10^{-6} M) at 298 K.

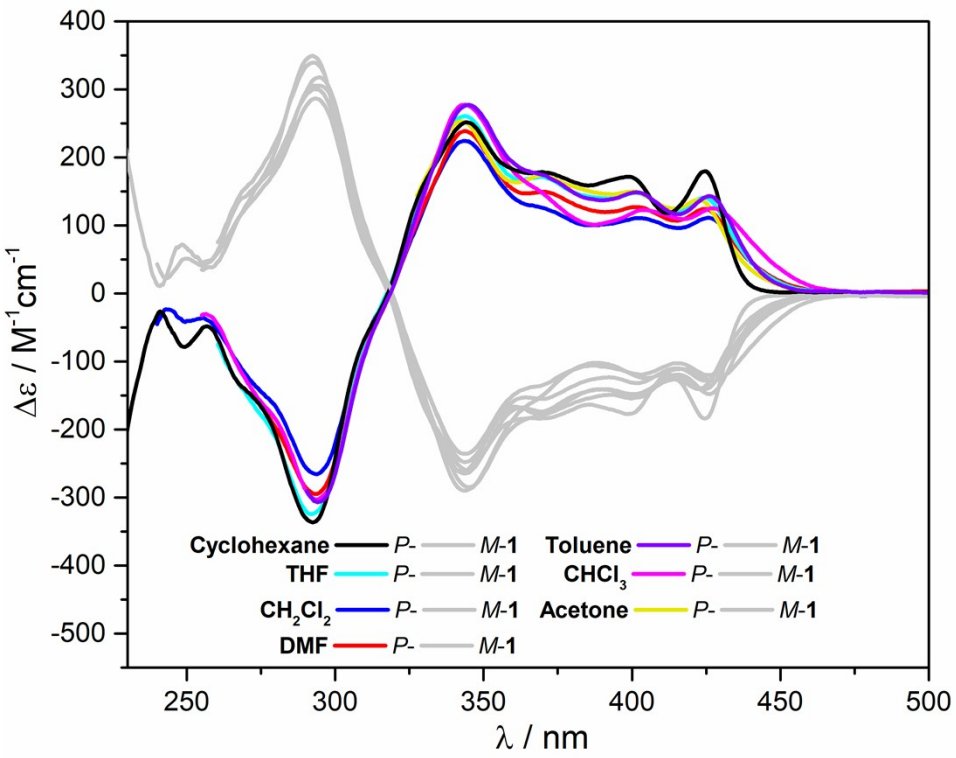

Figure S10. ECD spectra of **1** in cyclohexane (black), toluene (purple), THF (sky blue), $CHCl_3$ (pink), CH_2Cl_2 (blue), acetone (yellow), and DMF (red) solutions (~10^{-6} M) at 298 K.

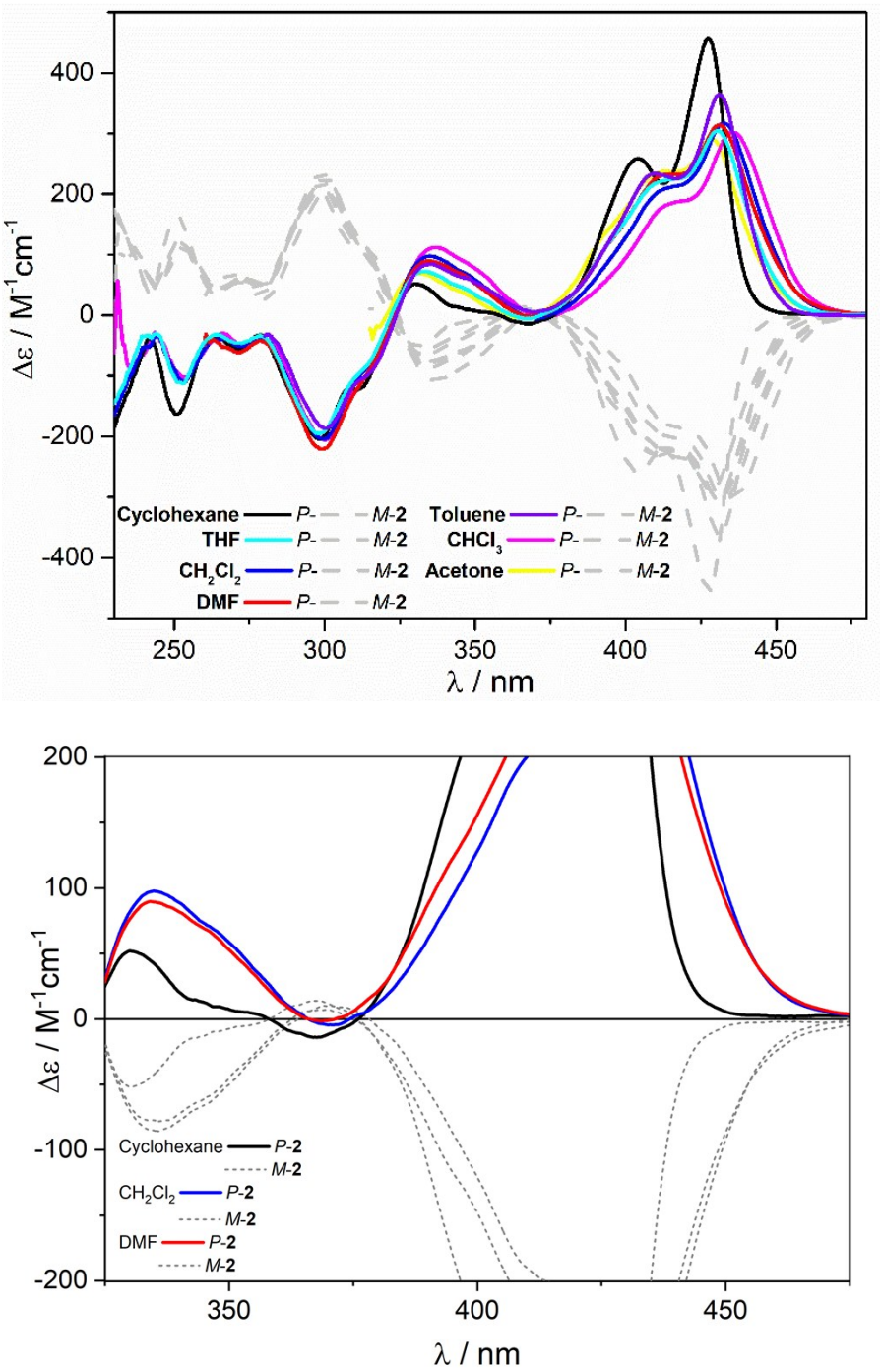

Figure S11. Top: ECD spectra of **2** in cyclohexane (black), toluene (purple), THF (sky blue), $CHCl_3$ (pink), CH_2Cl_2 (blue), acetone (yellow), and DMF (red) solutions (~10^{-6} M) at 298 K. Bottom: Enlargement of low-energy region of the ECD spectra (with bisignate signal) for cyclohexane, CH_2Cl_2, and DMF.

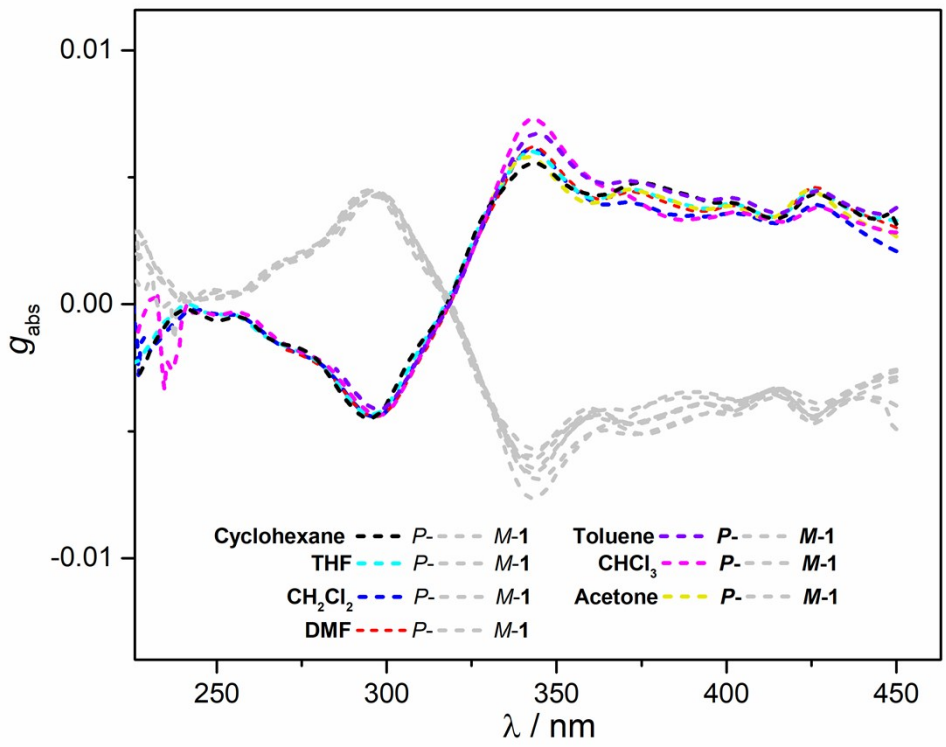

Figure S12. Absorption dissymmetry factor g_{abs} spectra of **1** in cyclohexane (black), toluene (purple), THF (sky blue), $CHCl_3$ (pink), CH_2Cl_2 (blue), acetone (yellow), and DMF (red) solutions (~10^{-6} M) at 298 K.

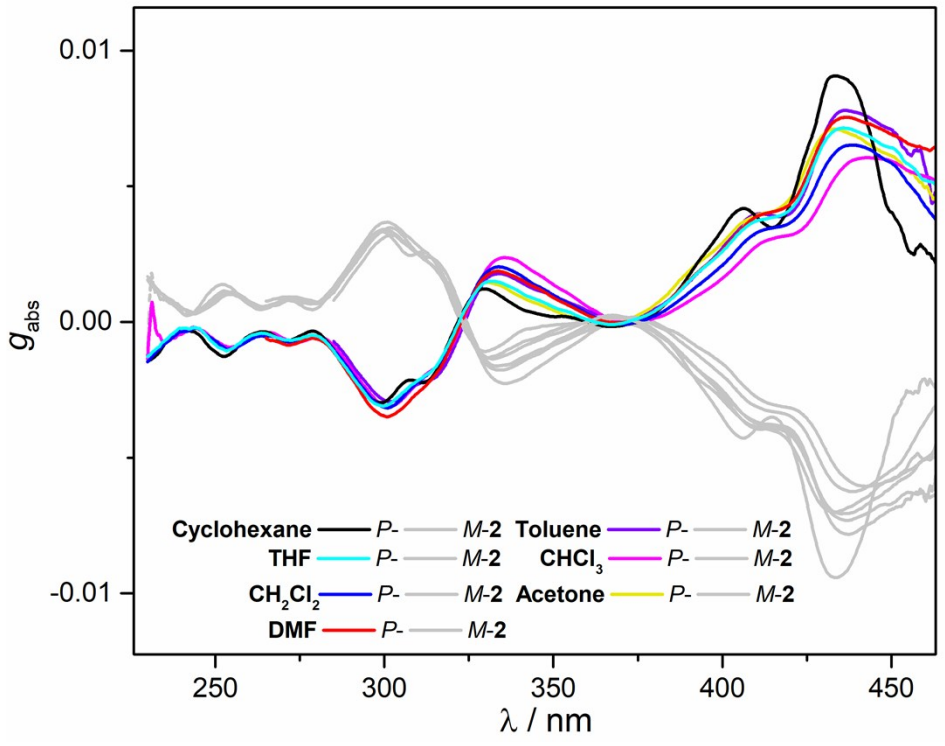

Figure S13. Absorption dissymmetry factor g_{abs} spectra of **2** in cyclohexane (black), toluene (purple), THF (sky blue), $CHCl_3$ (pink), CH_2Cl_2 (blue), acetone (yellow), and DMF (red) solutions (~10^{-6} M) at 298 K.

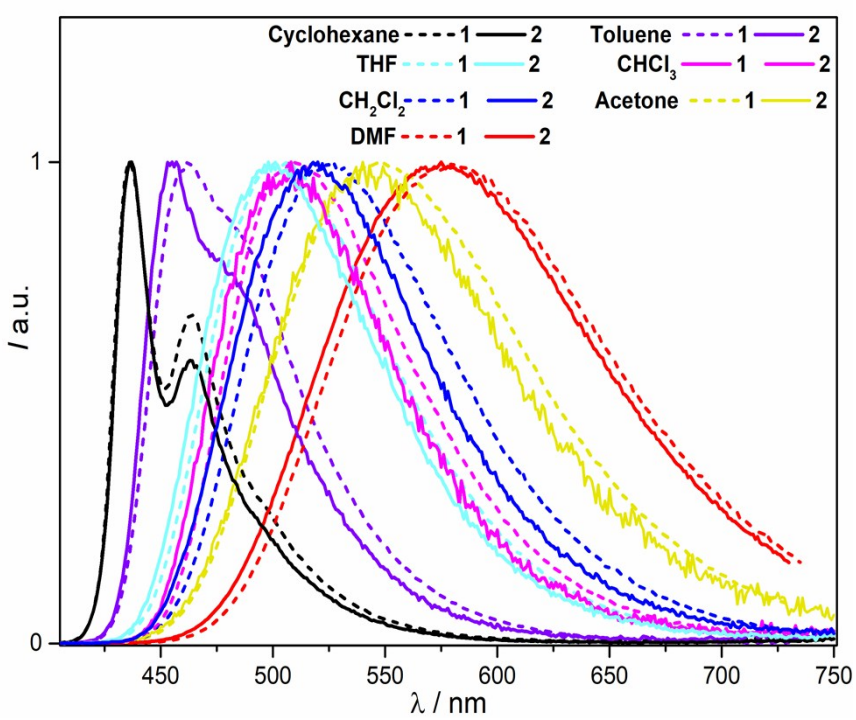

Figure S14. Normalized emission spectra of **1** (dashed lines) and **2** (solid lines) in cyclohexane (black), toluene (purple), THF (sky blue), $CHCl_3$ (pink), CH_2Cl_2 (blue), acetone (yellow), and DMF (red) solutions (~10^{-6} M) at 298 K.

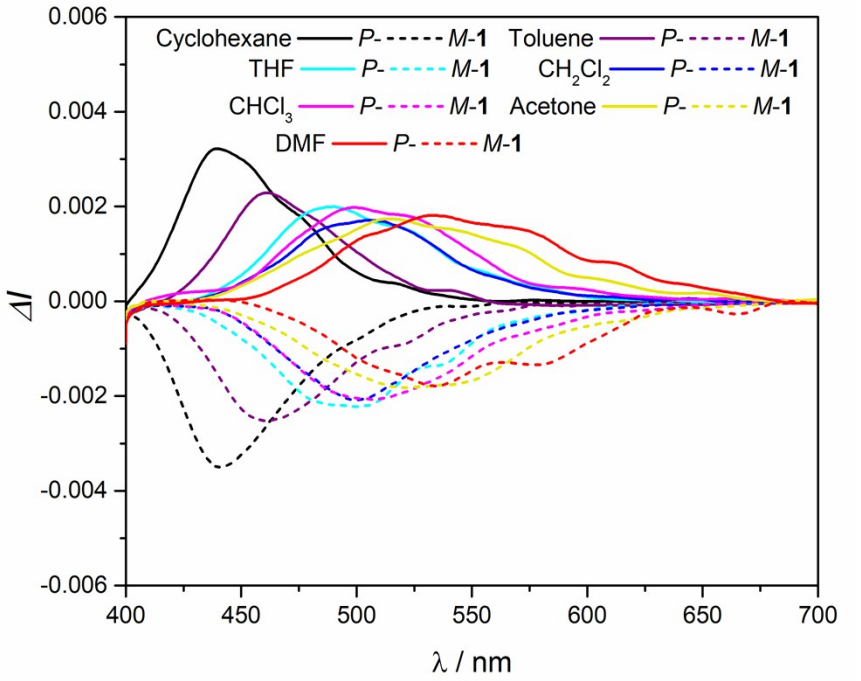

Figure S15. CPL spectra of *P*- and *M*-**1** (solid and dashed lines, respectively) in cyclohexane (black), toluene (purple), THF (sky blue), $CHCl_3$ (pink), CH_2Cl_2 (blue), acetone (yellow), and DMF (red) solutions (~10^{-6} M) at 298 K.

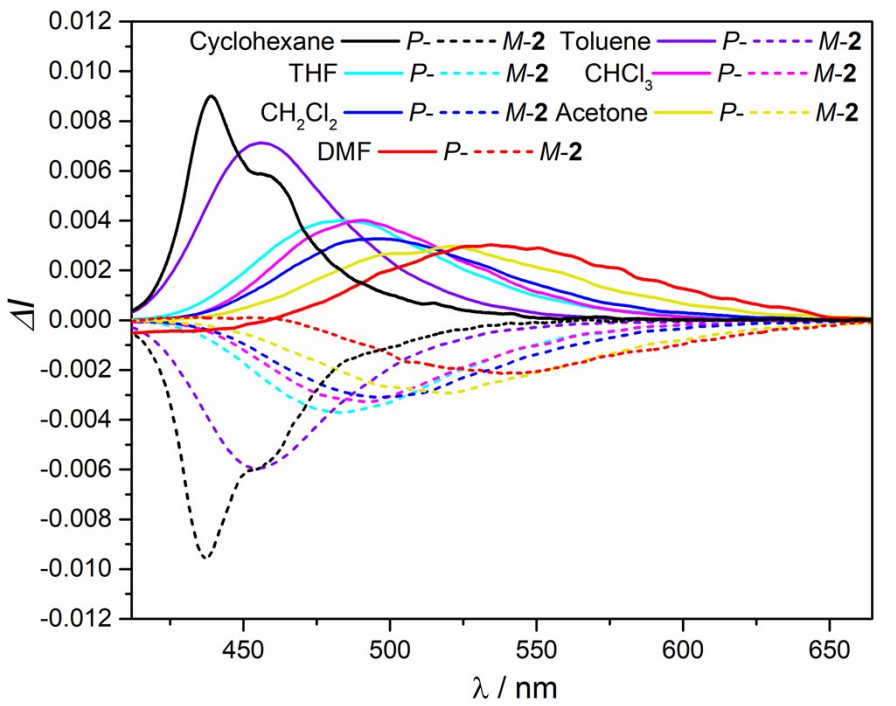

Figure S16. CPL spectra of *P*- and *M*-**2** (solid and dashed lines, respectively) in cyclohexane (black), toluene (purple), THF (sky blue), $CHCl_3$ (pink), CH_2Cl_2 (blue), acetone (yellow), and DMF (red) solutions (~10^{-6} M) at 298 K.

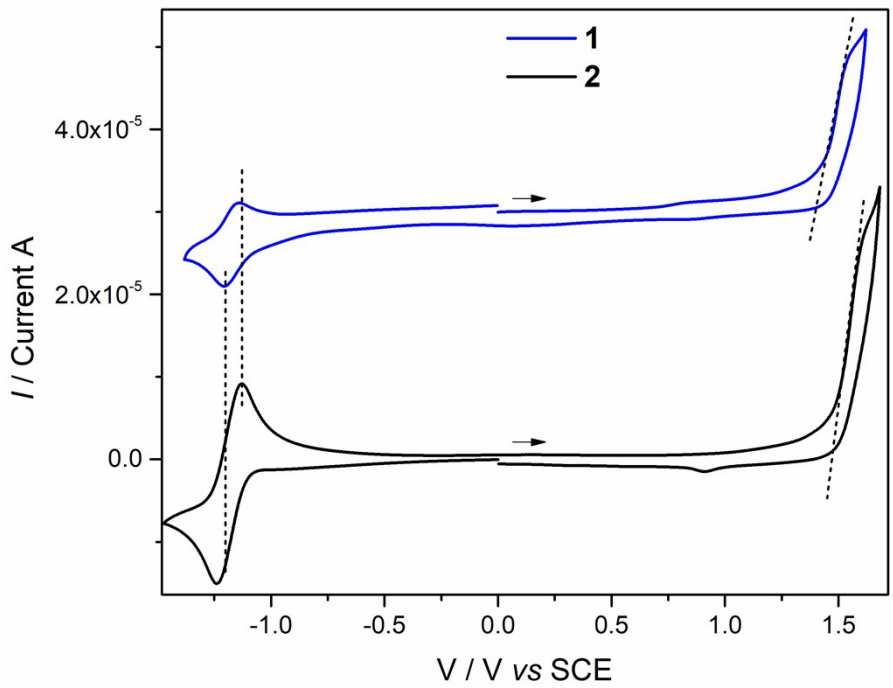

Figure S17. Cyclic voltammogram of **1** and **2** *versus* saturated calomel electrode (SCE) as the reference and 0.2 M Bu_4NPF_6 in CH_2Cl_2 as the electrolyte.

Table S2. Redox potentials (E_{Ox} and E_{Red}, in V) of **1** and **2** referenced *versus* saturated calomel electrode (SCE).

Compound	E_{Ox}	E_{Red}	HOMO[b] (eV)	LUMO[c] (eV)
1	1.39[a]	-1.18	-5.79	-3.22
2	1.47[a]	-1.19	-5.87	-3.21

[a] measured by differential pulse

[b] HOMO energy levels estimated from electrochemical results using the following equation:[5]
HOMO = -(E_{Ox} + 4.4) eV

[c] LUMO energy levels estimated from electrochemical results using the following equation:[5]
LUMO = -(E_{Red} + 4.4) eV

F. Computational part

[5] (a) C. M. Cardona, W. Li, A. E. Kaifer, D. Stockdale, G. C. Bazan, *Adv. Mater.* **2011**, *23*, 2367-2371; (b) A. J. Bard, L. R. Faulkner, *Electrochemical Methods: Fundamentals and Applications*, Wiley, New York, 2001.

Computational details

The computational protocol employed in these studies was based on the successful approach used in our preceding research on helicene derivatives functionalized by electron push-pull groups, presented in References 6 and 7. The molecular structures of truncated systems (with *n*-hexyl groups replaced by methyls) of **NPhBr**, **1** and **2** were optimized using density functional theory (DFT) with the BP[8] exchange-correlation functional and a split-valence basis set with one set of polarization functions for non-hydrogen atoms, SV(P).[9] The subsequent time-dependent DFT (TDDFT) linear response calculations of 120 (for **NPhBr**, **1**) and 150 (for **2**) lowest singlet excitation energies along with the associated dipole and rotatory strengths were performed at the BHLYP[10]/SV(P) level. The aforementioned computations employed the Turbomole package, version 6.6 (TM6.6)[11] and included solvent effects via the conductor-like screening model (COSMO) for dichloromethane (CH_2Cl_2 = DCM, $\varepsilon = 8.9$) with the default parameters of the TM6.6/COSMO implementation.[12] The simulated UV-vis and ECD spectra shown were obtained as the sums of Gaussian functions (with the root mean square width of $\sigma = 0.2$ eV) centered at the vertical excitation energies and scaled using the calculated dipole and rotatory strengths.[13] Simulated spectra for the helicene-TMS precursor **H6(TMS)$_2$** were taken from Reference 6.

To study the solvent-dependent fluorescence behaviour of **1** and **2**, electronic emission spectra via TDDFT S_1 excited-state modeling were obtained using the Gaussian program, version 09,[14] at the BHLYP/SV(P) level employing polarizable continuum solvent model for cyclohexane ($\varepsilon = 2.0$), dichloromethane ($\varepsilon = 8.9$), and *N*,*N*-dimethylformamide (DMF, $\varepsilon = 37.2$) with the default parameters of the G09/PCM implementation.[15] Following the procedure described in Reference 16, the calculations involved: (*i*) TDDFT S_1 excited-state geometry optimizations with linear response solvation model, LR-PCM, in which solvent reaction field is defined using the ground-state electron density, (*ii*) TDDFT S_1 excited-state energy calculations at S_1 TDDFT LR-PCM optimized geometries (from point (*i*)) with state-specific solvation approach, SS-PCM,[17] in which electrostatic potential

---

[6] K. Dhbaibi, L. Favereau, M. Srebro-Hooper, M. Jean, N. Vanthuyne, F. Zinna, B. Jamoussi, L. Di Bari, J. Autschbach, J. Crassous, *Chem. Sci.* **2018**, *9*, 735-742.

[7] R. Bouvier, R. Durand, L. Favereau, M. Srebro-Hooper, V. Dorcet, T. Roisnel, N. Vanthuyne, Y. Vesga, J. Donnelly, F. Hernandez, J. Autschbach, Y. Trolez, J. Crassous, *Chem. Eur. J.* **2018**, *24*, 14484-14494.

[8] a) A. D. Becke, *Phys. Rev. A* **1988**, *38*, 3098-3100; b) J. P. Perdew, *Phys. Rev. B* **1986**, *33*, 8822-8824; c) J. P. Perdew, *Phys. Rev. B* **1986**, *34*, 7406.

[9] a) A. Schäfer, H. Horn, R. Ahlrichs, *J. Chem. Phys.* **1992**, *97*, 2571-2577; b) K. Eichkorn, F. Weigend, O. Treutler, R. Ahlrichs, *Theor. Chem. Acc.* **1997**, *97*, 119-124; c) F. Weigend, R. Ahlrichs, *Phys. Chem. Chem. Phys.* **2005**, *7*, 3297-3305.

[10] a) A. D. Becke, *J. Chem. Phys.* **1993**, *98*, 1372-1377; b) C. Lee, W. Yang, R. G. Parr, *Phys. Rev. B* **1988**, *37*, 785-789.

[11] a) TURBOMOLE V6.6 2014, a development of University of Karlsruhe and Forschungszentrum Karlsruhe GmbH, 1989-2007, TURBOMOLE GmbH, since 2007; available from http://www.turbomole.com; b) R. Ahlrichs, M. Bär, M. Häser, H. Horn, C. Kölmel, *Chem. Phys. Lett.* **1989**, *162*, 165-169; c) F. Furche, R. Ahlrichs, C. Hättig, W. Klopper, M. Sierka, F. Weigend, *WIREs Comput. Mol. Sci.* **2014**, *4*, 91-100.

[12] a) A. Klamt, G. J. Schüürmann, *J. Chem. Soc., Perkin Trans. 2* **1993**, 799-805; b) A. Klamt, *J. Phys. Chem.* **1996**, *100*, 3349-3353.

[13] J. Autschbach, T. Ziegler, S. J. A. van Gisbergen, E. J. Baerends, *J. Chem. Phys.* **2002**, *116*, 6930-6940.

[14] Gaussian 09, Revision D.01., M. J. Frisch, G. W. Trucks, H. B. Schlegel, G. E. Scuseria, M. A. Robb, J. R. Cheeseman, G. Scalmani, V. Barone, B. Mennucci, G. A. Petersson, *et al.* Gaussian, Inc., Wallingford CT, 2009.

[15] a) M. Cossi, V. Barone, *J. Chem. Phys.* **2001**, *115*, 4708-4717; b) G. Scalmani, M. J. Frisch, B. Mennucci, J. Tomasi, R. Cammi, V. Barone, *J. Chem. Phys.* **2006**, *124*, 094107.

[16] J. B. Foresman, Æ Frisch, *Exploring Chemistry with Electronic Structure Methods*, 3rd ed., Gaussian, Inc.: Wallingford, CT, 2015, pp. 371-380.

[17] a) R. Improta, V. Barone, G. Scalmani, M. J. Frisch, *J. Chem. Phys.* **2006**, *125*, 054103; b) R. Improta, G. Scalmani, M. J. Frisch, V. Barone, *J. Chem. Phys.* **2007**, *127*, 074504.

generated by the excited-state electron density is being self-consistently converged with the solvent reaction field, and (*iii*) DFT S_0 ground-state energy calculations at S_1 TDDFT LR-PCM optimized geometries (from point (*i*)) with the static solvation from the excited state (from point (*ii*)). The difference between the energies calculated at points (*ii*) and (*iii*) corresponds to the vertical emission energy including the state-specific solvation correction.

The Onsager cavity radii, a_0, used to estimate the difference of dipole moments between the excited and ground states based on the Lippert-Mataga equation, were determined as described in the G09 manual via BHLYP/SV(P) calculations (employing G09) at BP/SV(P)-optimized (employing TM6.6) gas-phase geometries. The ground-state dipole moments were calculated with BHLYP/SV(P) (employing G09) at BP/SV(P)-optimized (employing TM6.6) geometries.

All calculations were performed without imposing symmetry.

Additional computed data

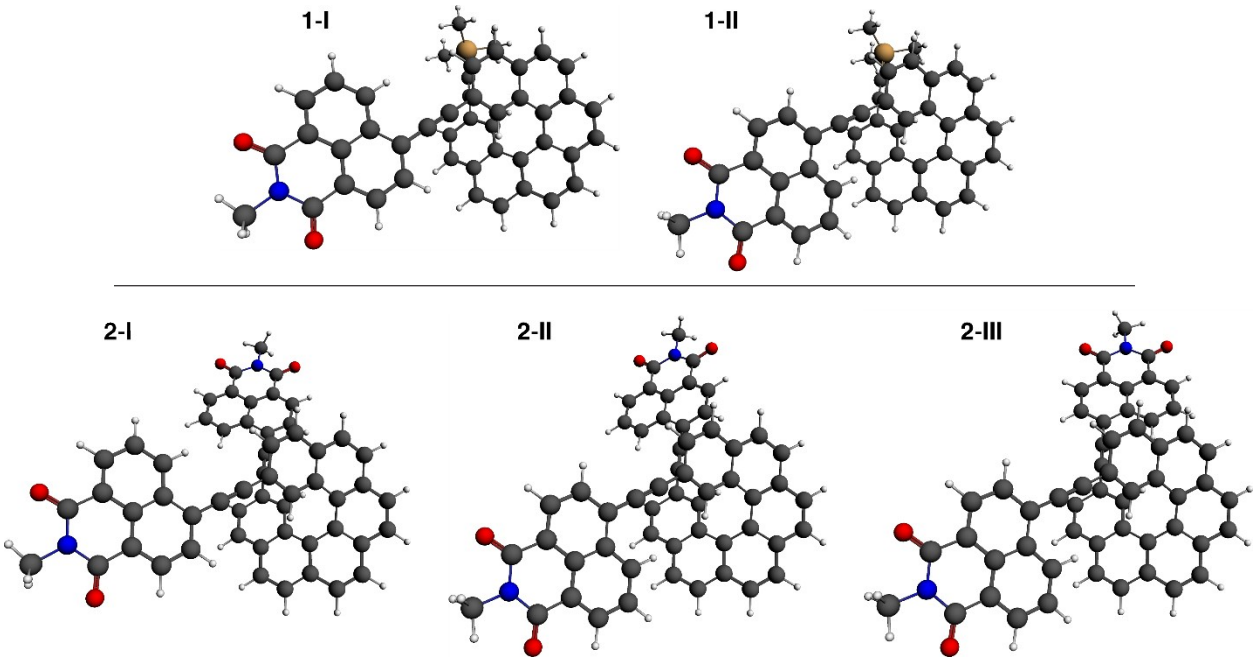

Figure S18. Selected low-energy optimized rotameric structures of helicene-naphthalimide derivatives **1** and **2** studied computationally. BP/SV(P) with dichloromethane continuum solvent model calculations. Compare with Table S3.

Table S3. Relative energies (ΔE in kcal/mol) and the corresponding Boltzmann populations (n_B in %, 25ºC) of the conformers of **1** and **2** shown in Figure S18. BP/SV(P) with dichloromethane continuum solvent model calculations.

System	ΔE	n_B
1-I	0.00	56
1-II	0.14	44
2-I	0.00	36
2-II	0.02	35
2-III	0.14	29

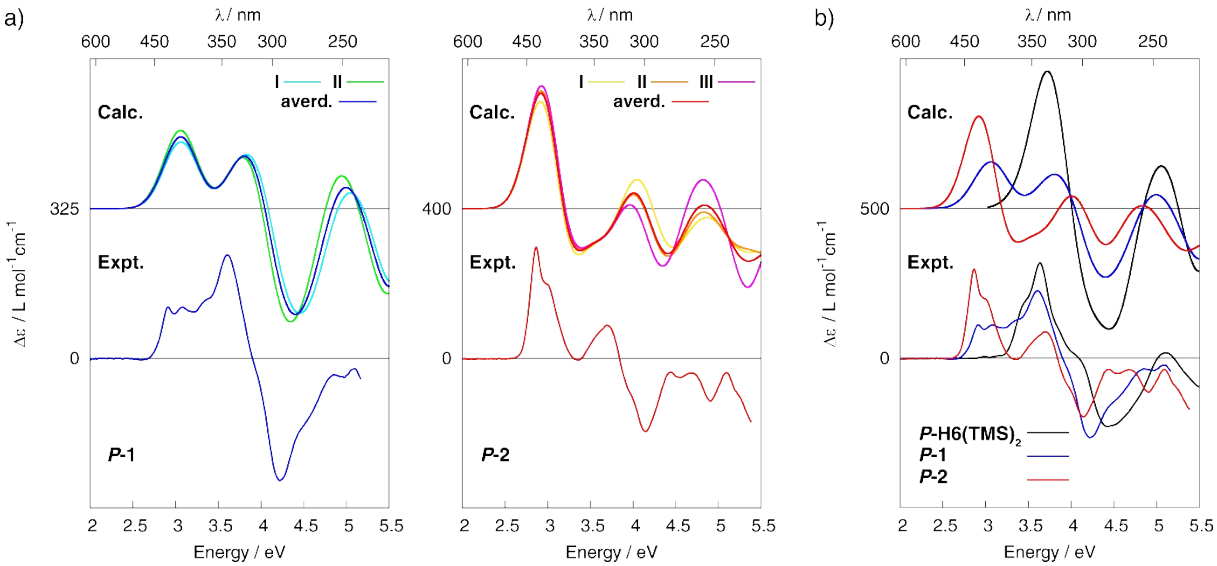

Figure S19. Comparison of the experimental and calculated TDDFT (BHLYP/SV(P) with dichloromethane continuum solvent model) ECD spectra of helicene-naphthalimide derivatives with the helicene-TMS system used as a reference. No spectral shift has been applied. Panel a: Numbers listed (I, II, III) refer to different conformers of *P*-**1** and *P*-**2** examined (see Figure S18). 'averd.' indicates Boltzmann-averaged (25°C) spectrum. Panel b: Simulated spectra of *P*-**1** and *P*-**2** correspond to Boltzmann-averaged (25°C) spectra from panel a.

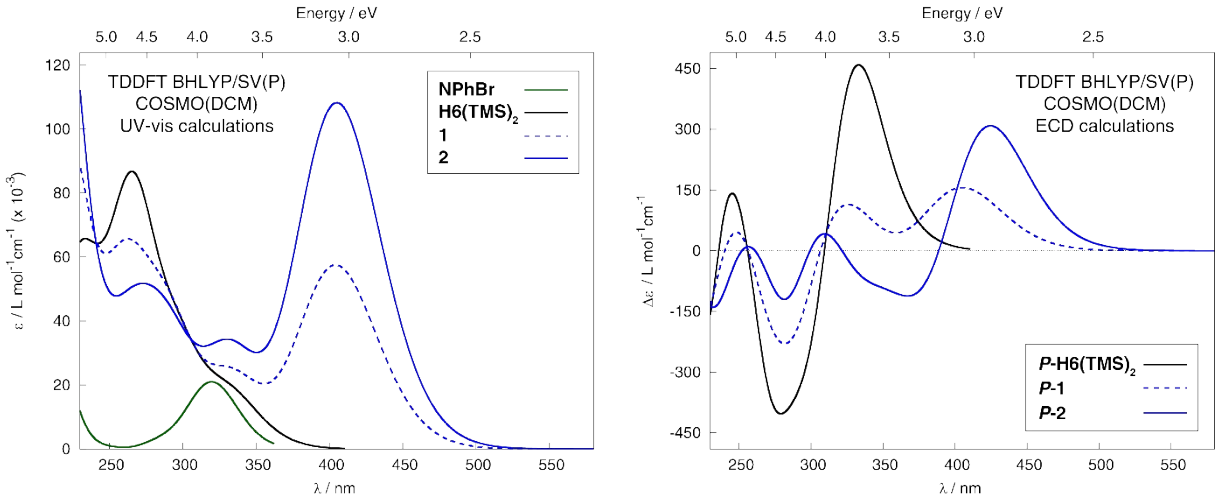

Figure S20. Comparison of the simulated UV-vis (left) and ECD (right) spectra of **1** and **2** (Boltzmann-averaged (25°C) spectra) with **H6(TMS)$_2$** and **NPhBr** systems used as references. No spectral shift has been applied.

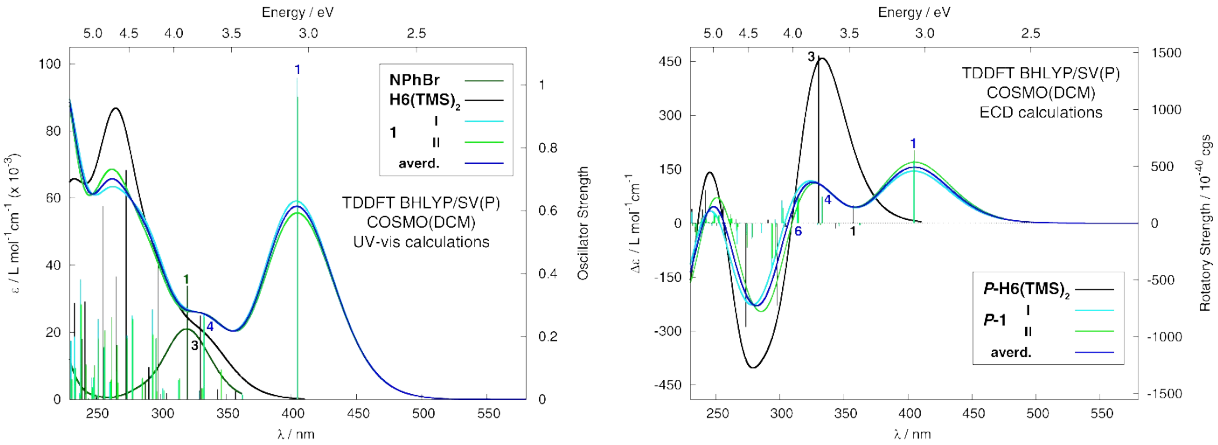

Figure S21. Comparison of the simulated UV-vis (left) and ECD (right) spectra of **1** with **H6(TMS)$_2$** and **NPhBr** used as references. No spectral shift has been applied. Calculated excitation energies and oscillator / rotatory strengths indicated as 'stick' spectra. Numbered excitations correspond to those analyzed in detail. 'averd.' indicates Boltzmann-averaged (25°C) spectrum. For the assignment of the calculated spectra of **H6(TMS)$_2$** see Ref. 6.

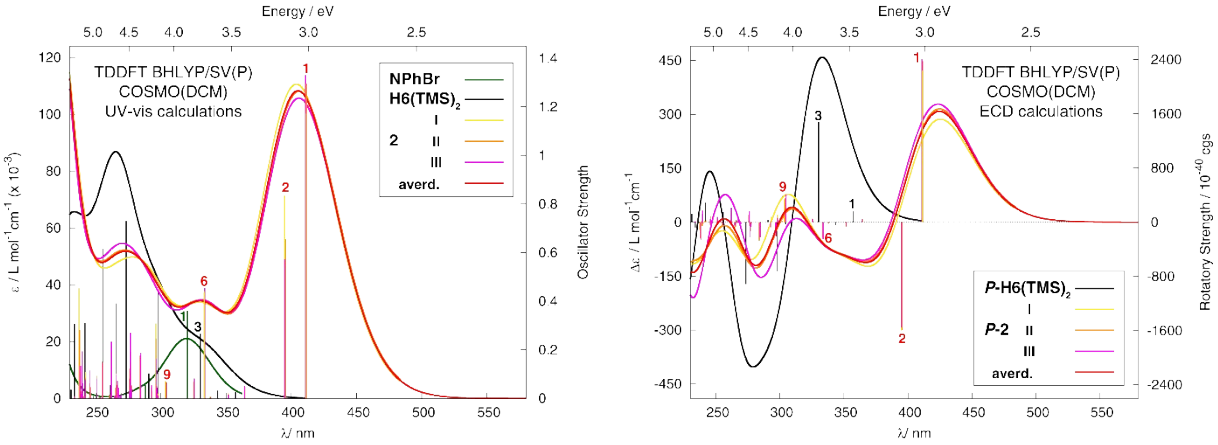

Figure S22. Comparison of the simulated UV-vis (left) and ECD (right) spectra of **2** with **H6(TMS)$_2$** and **NPhBr** used as references. No spectral shift has been applied. Calculated excitation energies and oscillator / rotatory strengths indicated as 'stick' spectra. Numbered excitations correspond to those analyzed in detail. 'averd.' indicates Boltzmann-averaged (25°C) spectrum. For the assignment of the calculated spectra of **H6(TMS)$_2$** see Ref. 6.

Table S4. Selected dominant excitations and occupied (occ) – unoccupied (unocc) MO pair contributions (greater than 10%) of **NPhBr**.

Excitation	*E* / eV	λ / nm	*f*	occ no.	unocc no.	%
1	3.87	320	0.361	0.06	72	73

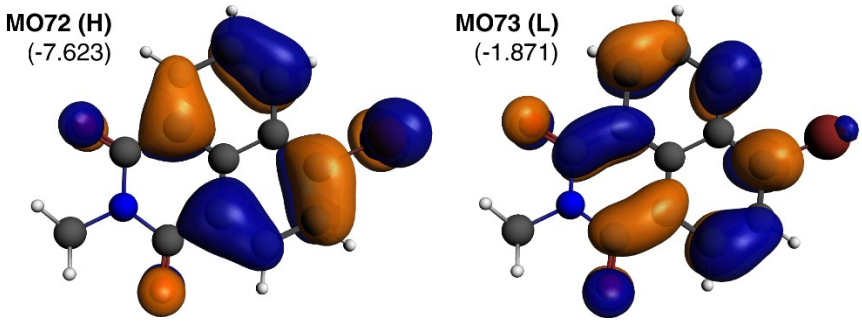

Figure S23. Isosurfaces (±0.03 au) of MOs involved in selected transitions of **NPhBr**. 'H' = HOMO, 'L' = LUMO. Values listed in the parentheses are the corresponding orbital energies, in eV.

Table S5. Selected dominant excitations and occupied (occ) – unoccupied (unocc) MO pair contributions (greater than 10%) of *P*-**1-I**.

Excitation	*E* / eV	λ / nm	*f*	*R* / 10^{-40} cgs	occ no.	unocc no.	%
1	3.07	404	1.023	548.80	172	173	66.0
					170	173	16.4
4	3.72	333	0.273	238.29	172	174	25.4
					171	175	15.8
					171	174	15.5
					171	173	14.9
					170	173	10.5
6	3.96	313	0.062	197.27	171	175	22.2
					171	176	11.5

Table S6. Selected dominant excitations and occupied (occ) – unoccupied (unocc) MO pair contributions (greater than 10%) of *P*-**1-II**.

Excitation	*E* / eV	λ / nm	*F*	*R* / 10^{-40} cgs	occ no.	unocc no.	%
1	3.06	405	0.962	643.16	172	173	67.1
					170	173	15.7
4	3.72	333	0.261	235.25	172	174	24.9
					171	174	18.4
					171	173	14.6
					171	175	14.1
					170	173	10.8
6	3.94	314	0.067	255.77	171	175	23.7
					171	176	10.3

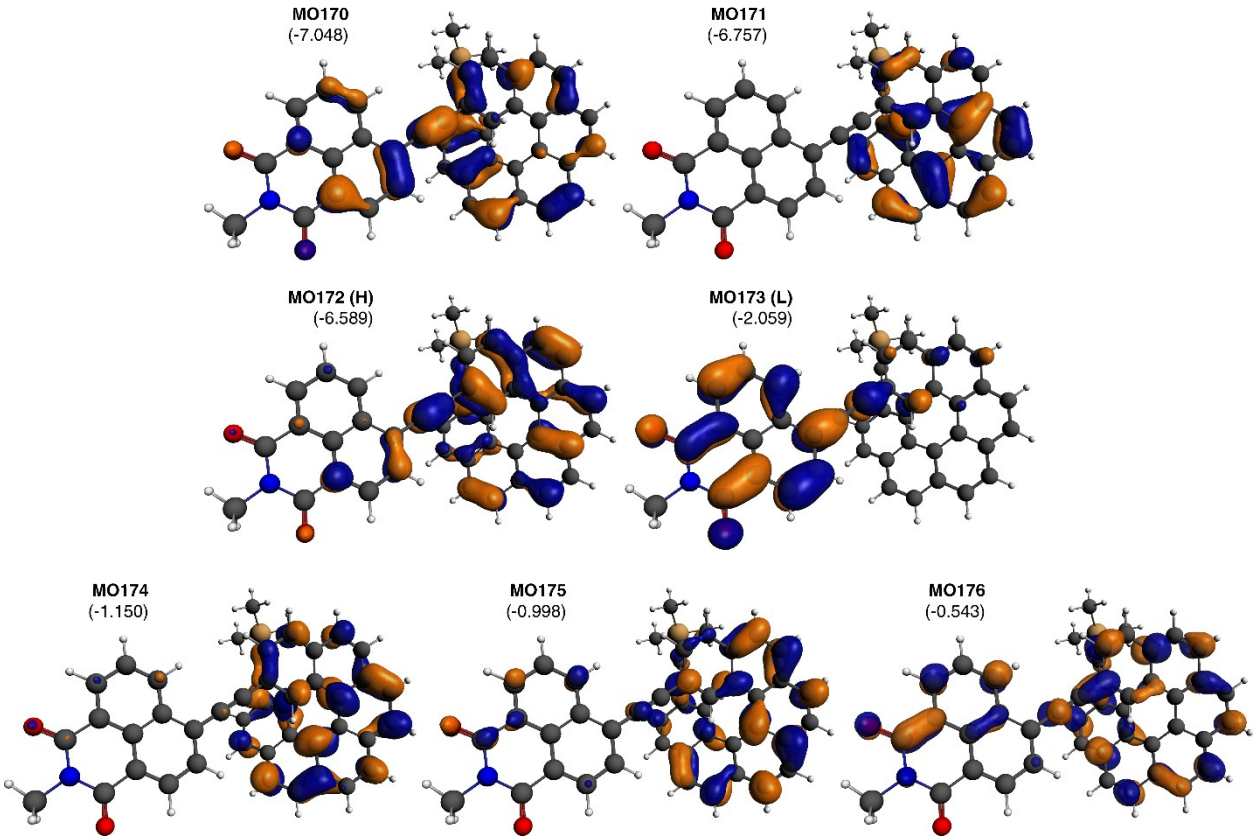

Figure S24. Isosurfaces (±0.03 au) of MOs involved in selected transitions of *P*-**1-I**. 'H' = HOMO, 'L' = LUMO. Values listed in the parentheses are the corresponding orbital energies, in eV. Isosurfaces of the corresponding MOs for conformer II appeared to be very similar and therefore they are not shown.

Table S7. Selected dominant excitations and occupied (occ) – unoccupied (unocc) MO pair contributions (greater than 10%) of *P*-**2-I**.

Excitation	E / eV	λ / nm	f	R / 10^{-40} cgs	occ no.	unocc no.	%
1	3.02	411	1.172	2239.09	206	207	56.4
					205	208	14.0
					204	208	13.2
2	3.14	395	0.836	-1596.90	206	208	49.3
					205	207	19.3
					204	207	16.8
6	3.72	333	0.436	-226.14	204	208	41.8
					203	207	20.4
					205	210	10.8
9	4.09	303	0.071	337.61	205	210	41.8
					204	208	17.6
					205	208	17.0

Table S8. Selected dominant excitations and occupied (occ) – unoccupied (unocc) MO pair contributions (greater than 10%) of *P*-**2-II**.

Excitation	*E* / eV	λ / nm	*f*	*R* / 10^{-40} cgs	occ no.	unocc no.	%
1	3.01	411	1.296	2375.87	206	207	56.5
					205	208	15.0
					204	208	12.4
2	3.13	396	0.654	-1589.94	206	208	48.8
					205	207	20.9
					204	207	16.0
6	3.72	333	0.443	-224.56	204	208	42.0
					203	207	20.7
					205	210	10.4
9	4.08	304	0.068	356.88	205	210	41.1
					204	208	18.7
					205	208	14.7

Table S9. Selected dominant excitations and occupied (occ) – unoccupied (unocc) MO pair contributions (greater than 10%) of *P*-**2-III**.

Excitation	*E* / eV	λ / nm	*f*	*R* / 10^{-40} cgs	occ no.	unocc no.	%
1	3.02	411	1.330	2404.62	206	207	57.0
					205	208	14.5
					204	208	12.5
2	3.14	395	0.572	-1555.58	206	208	48.8
					205	207	20.6
					204	207	16.1
6	3.72	334	0.453	-246.95	204	208	41.4
					203	207	21.5
					205	210	11.1
					206	207	10.0
9	4.07	305	0.066	404.82	205	210	42.1
					204	208	19.9
					205	208	15.4

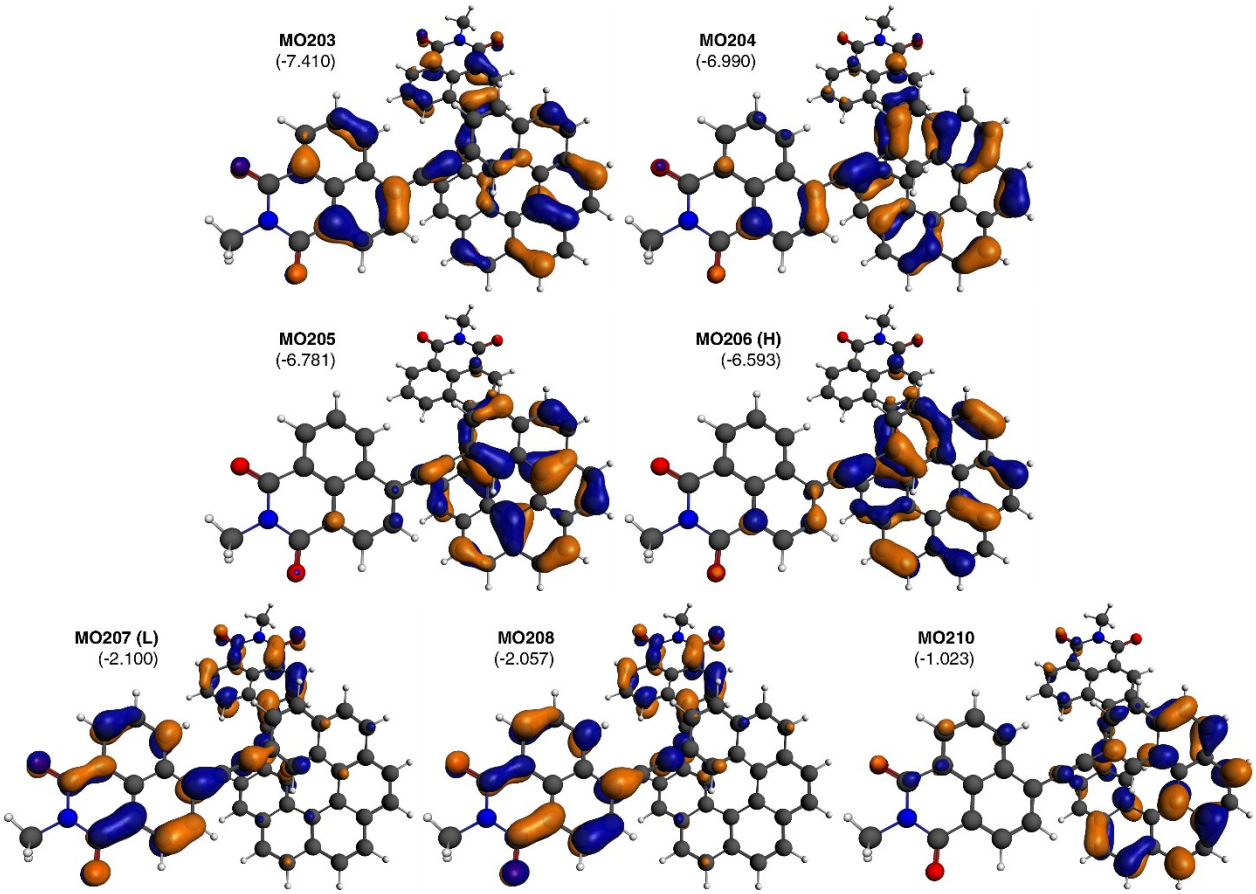

Figure S25. Isosurfaces (±0.03 au) of MOs involved in selected transitions of *P*-**2-I**. 'H' = HOMO, 'L' = LUMO. Values listed in the parentheses are the corresponding orbital energies, in eV. Isosurfaces of the corresponding MOs for conformers II and III appeared to be very similar and therefore they are not shown.

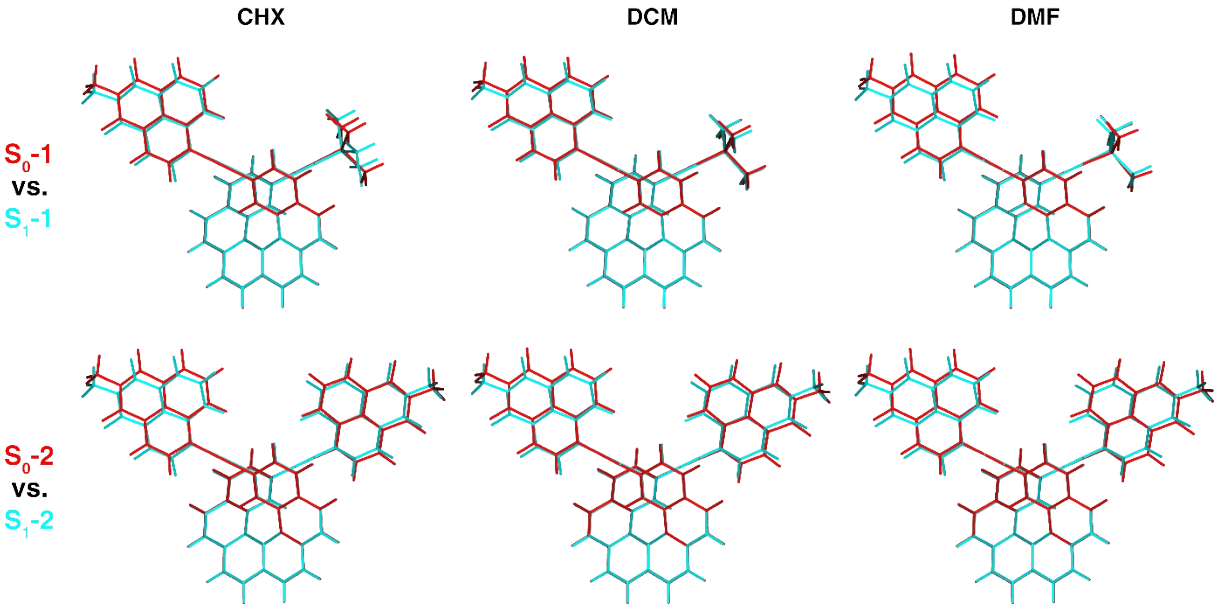

Figure S26. Overlays of optimized ground-state (S_0, red) and first singlet excited-state (S_1 based on TDDFT LR-PCM geometry optimization, blue) structures of helicene-naphthalimide derivatives **1** (conformer I, top) and **2** (conformer I, bottom). CHX, DCM, and DMF stand for cyclohexane, dichloromethane, and dimethylformamide solvent, respectively. Similarly small structural changes between ground and excited states of **1** and **2** involving primarily planarization of the naphthalimide groups with respect to the terminal rings of the helicene moiety were also observed for conformers II and III.

Table S10. Experimental and calculated (TDDFT BHLYP/SV(P) with continuum solvent model) photophysical data of helicene-naphthalimide derivative **1**.[a]

System / method	CHX		DCM		DMF	
	n_B	λ (f / R / g_{lum})	n_B	λ (f / R / g_{lum})	n_B	λ (f / R / g_{lum})
Expt.						
1	-	436	-	527	-	576
Calc. LR-PCM S_1[b]						
1-I	40	443 (1.190/450.25/1.6)	42	467 (1.425/341.96/1.0)	42	474 (1.495/304.47/0.8)
1-II	60	443 (1.082/464.57/1.8)	58	467 (1.331/355.50/1.1)	58	474 (1.403/315.87/0.9)
Calc. SS-PCM S_1[c]						
1-I	43	446 (0.988/498.40/2.1)	63	516 (0.924/444.13/1.8)	75	559 (0.875/417.83/1.6)
1-II	57	445 (0.877/519.07/2.5)	37	509 (0.830/477.19/2.1)	25	547 (0.790/456.12/2.0)

[a] λ – S_0-S_1 energy difference, in nm. f – oscillator strength. R – rotatory strength, in 10^{-40} cgs. g_{lum} – emission dissymmetry factor, in 10^{-3}. n_B – Boltzmann population at 25°C, in %. CHX, DCM, and DMF stand for cyclohexane, dichloromethane, and dimethylformamide solvent, respectively.

[b] S_1 properties at S_1 geometry obtained from TDDFT optimization using linear-response continuum solvent model approach (LR-PCM), corresponding to the emission process occurring in a solvent reaction field created in response to the S_0 electron density.

[c] S_1 properties at S_1 TDDFT LR-PCM optimized geometry computed by employing TDDFT with state-specific continuum solvent model approach (SS-PCM), corresponding to the emission process occurring in a solvent reaction field created in response to the S_1 electron density.

Table S11. Experimental and calculated (TDDFT BHLYP/SV(P) with continuum solvent model) photophysical data of helicene-naphthalimide derivative **2**.[a]

System / method	CHX		DCM		DMF	
	n_B	λ (f / R / g_{lum})	n_B	λ (f / R / g_{lum})	n_B	λ (f / R / g_{lum})
Expt.						
2	-	436	-	520	-	562
Calc. LR-PCM S_1[b]						
2-I	23	442 (1.216/764.60/2.7)	25	466 (1.446/518.03/1.4)	25	474 (1.515/452.65/1.2)
2-II	35	442 (1.123/788.53/3.0)	33	466 (1.357/531.56/1.6)	32	474 (1.428/450.61/1.3)
2-III	42	441 (1.161/793.24/2.9)	42	466 (1.378/534.40/1.6)	43	474 (1.439/448.19/1.2)
Calc. SS-PCM S_1[c]						
2-I	27	443 (1.024/857.23/3.5)	48	512 (0.957/694.35/2.7)	58	558 (0.907/637.86/2.4)
2-II	38	443 (0.928/881.69/4.0)	26	506 (0.873/732.13/3.1)	17	545 (0.830/678.63/2.8)
2-III	35	441 (0.971/877.65/3.9)	26	504 (0.906/722.01/3.0)	25	545 (0.855/663.66/2.7)

[a] λ – S_0-S_1 energy difference, in nm. f – oscillator strength. R – rotatory strength, in 10^{-40} cgs. g_{lum} – emission dissymmetry factor, in 10^{-3}. n_B – Boltzmann population at 25°C, in %. CHX, DCM, and DMF stand for cyclohexane, dichloromethane, and dimethylformamide solvent, respectively.

[b] S_1 properties at S_1 geometry obtained from TDDFT optimization using linear-response continuum solvent model approach (LR-PCM), corresponding to the emission process occurring in a solvent reaction field created in response to the S_0 electron density.

[c] S_1 properties at S_1 TDDFT LR-PCM optimized geometry computed by employing TDDFT with state-specific continuum solvent model approach (SS-PCM), corresponding to the emission process occurring in a solvent reaction field created in response to the S_1 electron density.

Table S12. Onsager cavity radii, a_0, and ground-state dipole moment values, μ_g, based on DFT calculations, along with slope values from the Lippert-Mataga plots, and the corresponding values of the difference between dipole moments of excited and ground states, $\Delta\mu_{eg}$, for helicene-naphthalimide derivatives **1** and **2**. For visualization of different conformers (of Boltzmann populations n_B, 25ºC) / models of **1** and **2** examined here see Figures S18 and S27. [a]

System	n_B / %	a_0 / Å	μ_g / D [b]	slope / cm^{-1}	$\Delta\mu_{eg}$ / D
1-I	48	6.86	6.30	15 870	22.6
1-II	52	6.80	6.48		22.3
1$^{TMS\rightarrow Me}$-I [c]	47	6.64	6.75		21.5
1$^{TMS\rightarrow Me}$-II [c]	53	6.60	6.91		21.3
2-I	32	7.20	5.89	14 140	22.9
2-II	33	7.17	6.06		22.8
2-III	36	7.19	6.42		22.9
2^{xray}-I [d]	60	7.84	6.02		26.0
2^{xray}-II [d]	40	7.57	6.12		27.7

[a] The corresponding Boltzmann populations (25ºC), n_B, for different conformers calculated using BP/SV(P). The Onsager cavity radii, a_0, and ground-state dipole moment values, μ_g, calculated using BHLYP/SV(P) at BP/SV(P)-optimized geometries. All the calculations correspond to gas-phase environment. Magnitudes of the difference of dipole moments between excited and ground states, $\Delta\mu_{eg}$, estimated using the Lippert-Mataga equation:

$$\Delta\mu_{eg} = ((\text{slope} \cdot h \cdot c \cdot a_0^3)/2)^{1/2}$$

where h is the Planck constant (= 6.6256×10^{-27} erg·s), c is the light velocity (= 2.9979×10^{10} cm/s), a_0 is the Onsager cavity radius (in Å). As it appears that for the systems studied here μ_g and μ_e vectors point in different directions, excited-state dipole moment values, μ_e, were not estimated.

Statistics that describe a linear trend for Lippert-Mataga plots, by fitting a straight line using the least square method, is presented below.

Equation: y = a + b*x for linear fits of Lippert-Mataga plots					
1			**2**		
Pearson's r Adj. R-Square	0.97662 0.94455		Pearson's r Adj. R-Square	0.98195 0.95707	
	Value	Standard Error		Value	Standard Error
Intercept	1043.8	306.2	Intercept	1010.4	238.7
Slope	15869.1	1562.0	Slope	14136.8	1217.7

[b] Compare with Figure S28.

[c] Helicene-naphthalimide derivative **1** corresponding to a model system with both *n*-hexyl and trimethylsilyl groups replaced by methyls.

[d] Helicene-naphthalimide derivative **2** corresponding to one of two different molecular structures of non-truncated molecule of **2** found in the X-ray crystal of the compound (compare with Section D).

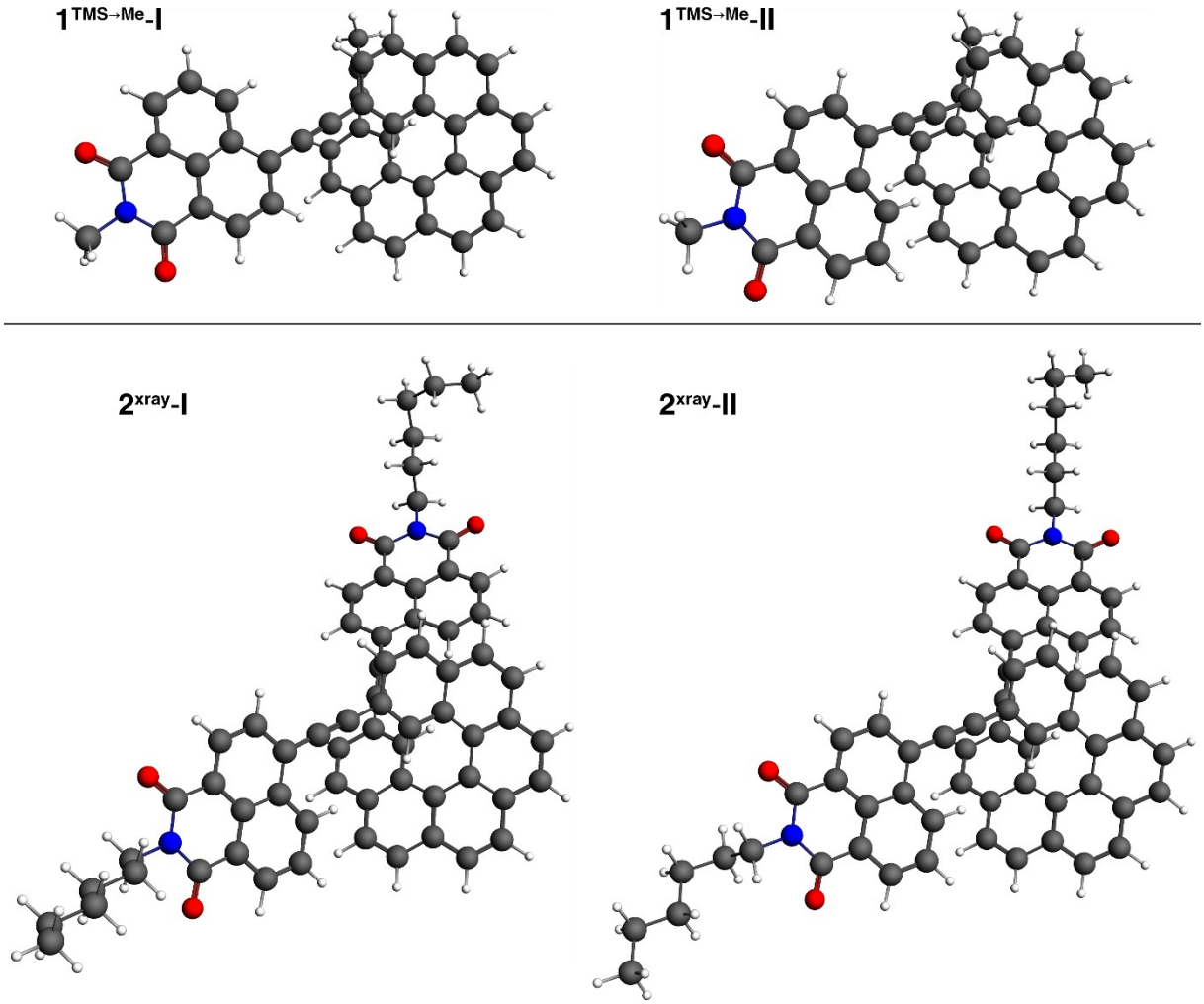

Figure S27. Additional computed models of helicene-naphthalimide derivatives **1** and **2**. BP/SV(P) gas-phase calculations.

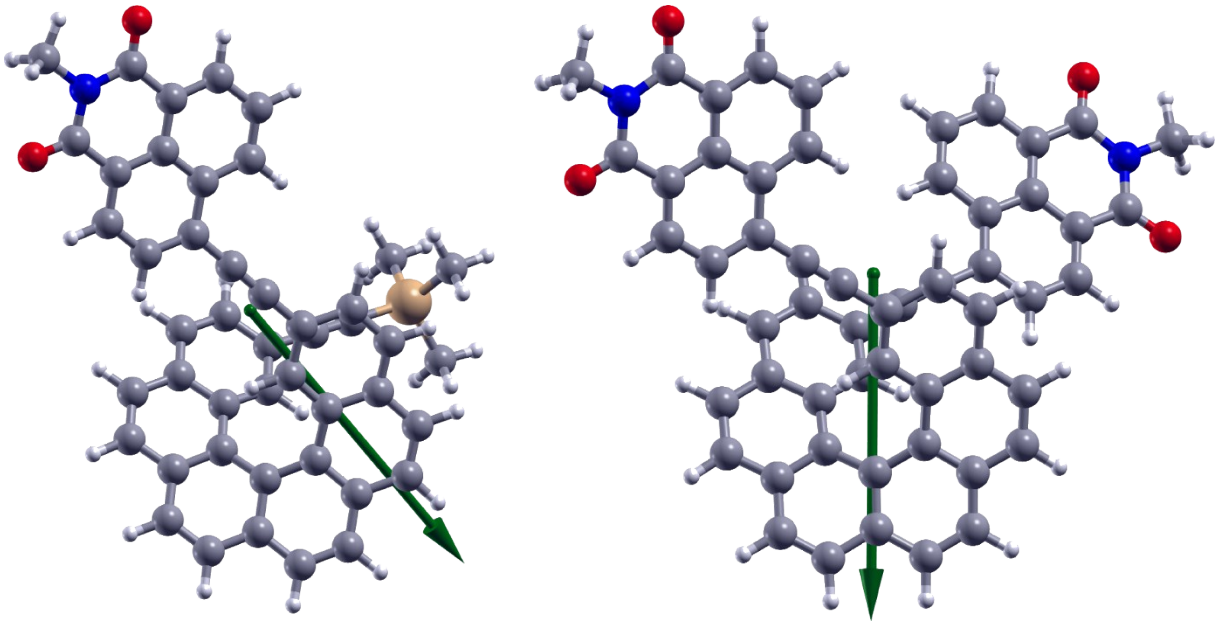

Figure S28. Ground-state dipole moment vectors μ_g (green vectors with origin located at the center of nuclear charge, scaled by a factor of 1.5, pointing from the negative to the positive pole of the dipole) for the helicene-naphthalimide derivatives **1** (conformer I, left) and **2** (conformer I, right) based on the BHLYP/SV(P) gas-phase calculations at BP/SV(P) gas-phase optimized geometries. The corresponding μ_g vectors for remaining conformers / models of **1** and **2** listed in Table S12 appeared to be very similar and therefore they are not shown. Compare with Table S12.

Table S13. S_1 excited-state dipole moment values for helicene-naphthalimide derivatives **1** and **2** based on the TDDFT BHLYP/SV(P) calculations with continuum solvent model.[a]

System	CHX		DCM		DMF	
	n_B	μ_e	n_B	μ_e	n_B	μ_e
1						
1-I	43	15.99 (7.03)	63	22.48 (7.78)	75	25.04 (8.11)
1-II	57	15.48	37	21.52	25	23.83
2						
2-I	27	13.52 (6.58)	48	19.98 (7.19)	58	22.63 (7.39)
2-II	38	12.58	26	18.32	17	20.74
2-III	35	12.45	26	18.44	25	21.07

[a] μ_e – S_1 excited-state dipole moment value, in D, based on the TDDFT BHLYP/SV(P) SS-PCM solvent calculation at S_1 TDDFT BHLYP/SV(P) LR-PCM solvent optimized geometry. For **1-I** and **2-I**, the corresponding values of ground-state dipole moment μ_g, in D, based on the BHLYP/SV(P) solvent calculations at S_0 BP/SV(P) solvent optimized geometries, are given in parentheses. n_B – Boltzmann population at 25°C, in %. Compare with Figures S29 and S30. CHX, DCM, and DMF stand for cyclohexane, dichloromethane, and dimethylformamide solvent, respectively.

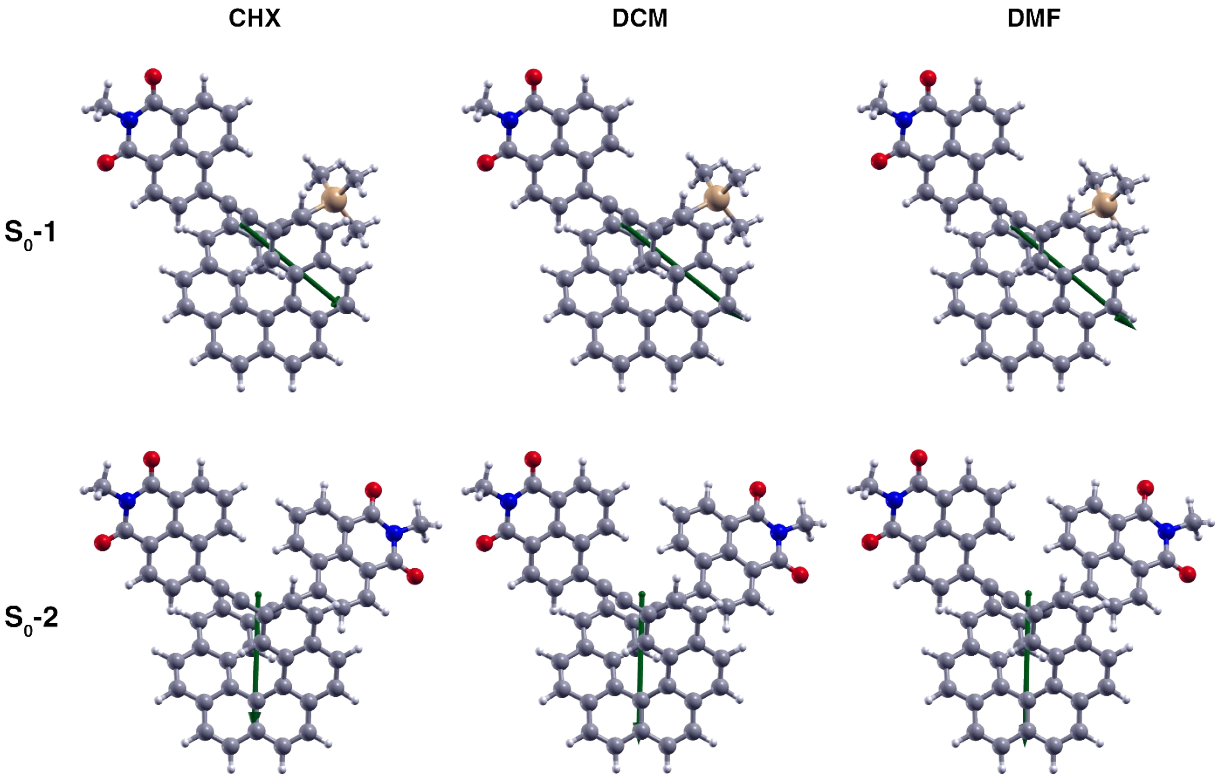

Figure S29. Ground-state dipole moment vectors μ_g (green vectors with origin located at the center of nuclear charge, not scaled, pointing from the negative to the positive pole of the dipole) for the helicene-naphthalimide derivatives **1** (conformer I) and **2** (conformer I) based on the BHLYP/SV(P) solvent calculations at S_0 BP/SV(P) solvent optimized geometries. The corresponding μ_g vectors for remaining conformers of **1** and **2** appeared to be very similar and therefore they are not shown. CHX, DCM, and DMF stand for cyclohexane, dichloromethane, and dimethylformamide solvent, respectively. Compare with Table S13.

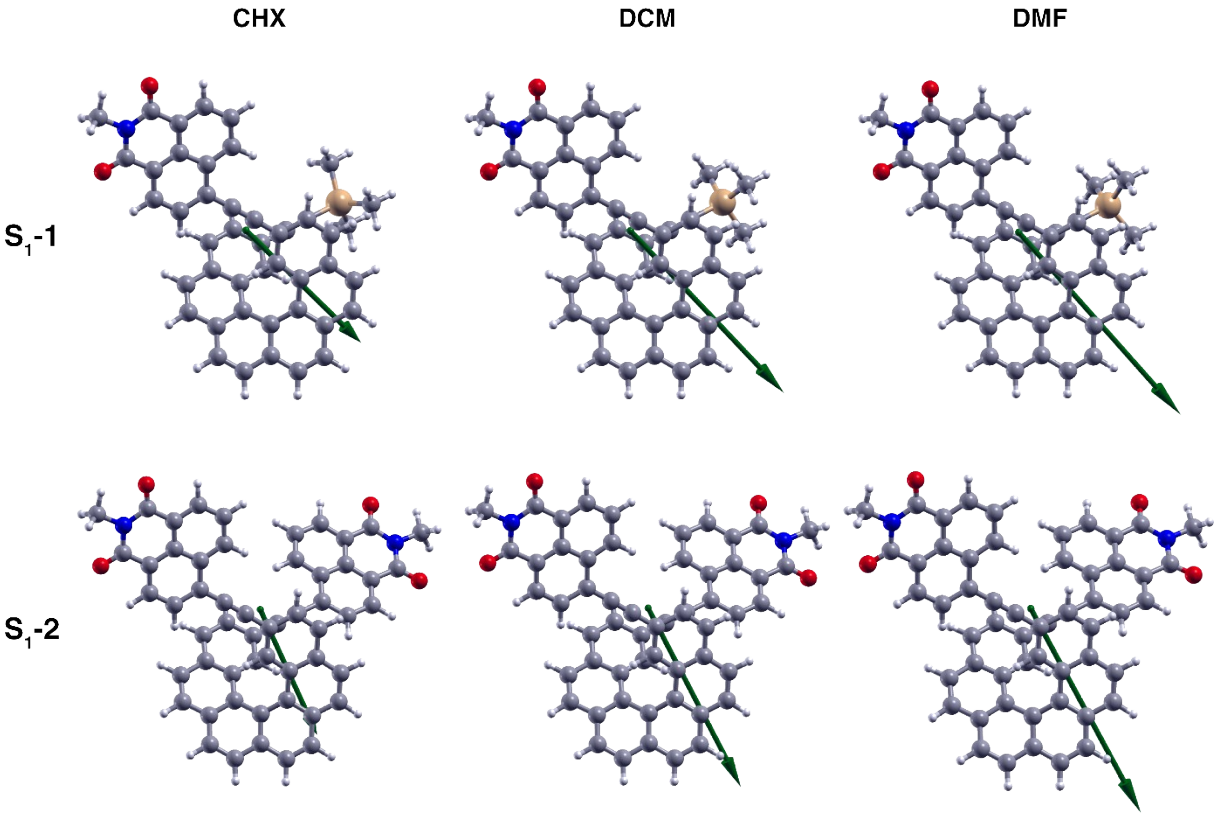

Figure S30. S_1 excited-state dipole moment vectors μ_e (green vectors with origin located at the center of nuclear charge, scaled by a factor of 0.5, pointing from the negative to the positive pole of the dipole) for the helicene-naphthalimide derivatives **1** (conformer I) and **2** (conformer I) based on the TDDFT BHLYP/SV(P) SS-PCM solvent calculations at S_1 TDDFT BHLYP/SV(P) LR-PCM solvent optimized geometries. The corresponding μ_e vectors for remaining conformers of **1** and **2** appeared to be very similar and therefore they are not shown. CHX, DCM, and DMF stand for cyclohexane, dichloromethane, and dimethylformamide solvent, respectively. Compare with Table S13.

Table S14. Values of the difference between dipole moments of the excited and ground states, $\Delta\mu_{eg}$ in D, for helicene-naphthalimide derivatives **1** and **2** based on the TDDFT BHLYP/SV(P) calculations with continuum solvent model.[a]

Solvent	**1-I**	**2-I**
CHX	9.051 / 8.706 / 8.716	8.581 / 7.987 / 7.997
DCM	14.869 / 14.255 / 12.546	14.733 / 13.714 /12.064
DMF	17.115 / 16.569 / 14.047	17.355 / 16.203 / 13.748

[a] Calculated as a magnitude of $\Delta\mu_{eg} = \mu_e - \mu_g$ vector with S_1 excited-state dipole moment vector μ_e obtained from the TDDFT BHLYP/SV(P) SS-PCM solvent calculation at S_1 TDDFT BHLYP/SV(P) LR-PCM solvent optimized geometry, and S_0 ground-state dipole moment vector μ_g obtained from the DFT BHLYP/SV(P) solvent calculations at S_0 BP/SV(P) solvent optimized geometry / S_1 TDDFT BHLYP/SV(P) LR-PCM solvent optimized geometry / S_1 TDDFT BHLYP/SV(P) LR-PCM solvent optimized geometry and with the static solvation from the excited state. Compare with Figures S29 and S30. CHX, DCM, and DMF stand for cyclohexane, dichloromethane, and dimethylformamide solvent, respectively.

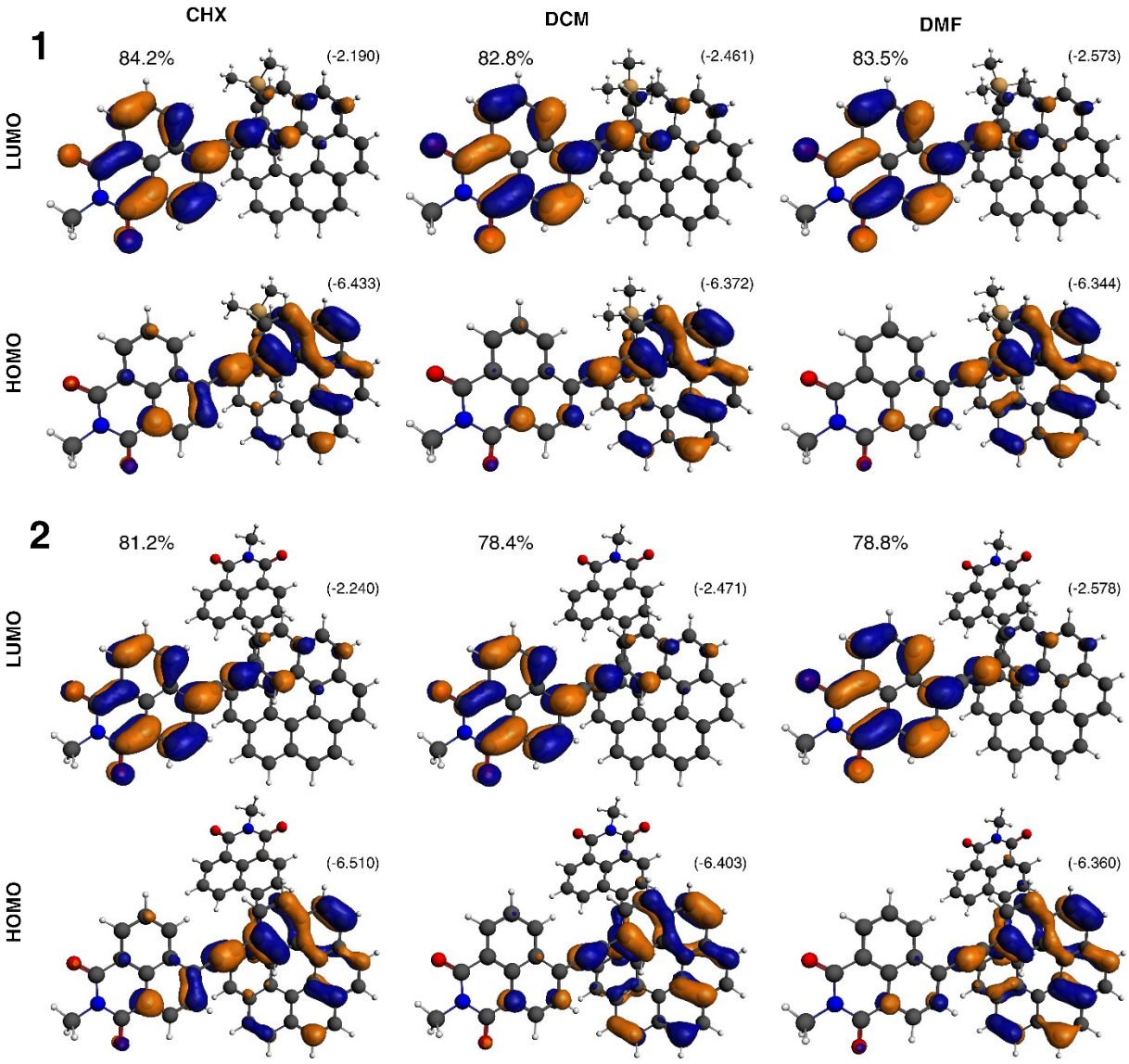

Figure S31. Isosurfaces (±0.03 au) of MOs predominantly involved in the $S_1 \rightarrow S_0$ transitions for the helicene-naphthalimide derivatives **1** (conformer I) and **2** (conformer I) based on the TDDFT BHLYP/SV(P) SS-PCM solvent calculations at S_1 TDDFT BHLYP/SV(P) LR-PCM solvent optimized geometries. Numbers listed in % refer to the HOMO-LUMO contributions to the emission transition, while values given in the parentheses are the corresponding orbital energies, in eV. Isosurfaces of the corresponding MOs for conformers II and III of S_1-**1** and S_1-**2** appeared to be very similar and therefore they are not shown. CHX, DCM, and DMF stand for cyclohexane, dichloromethane, and dimethylformamide solvent, respectively.

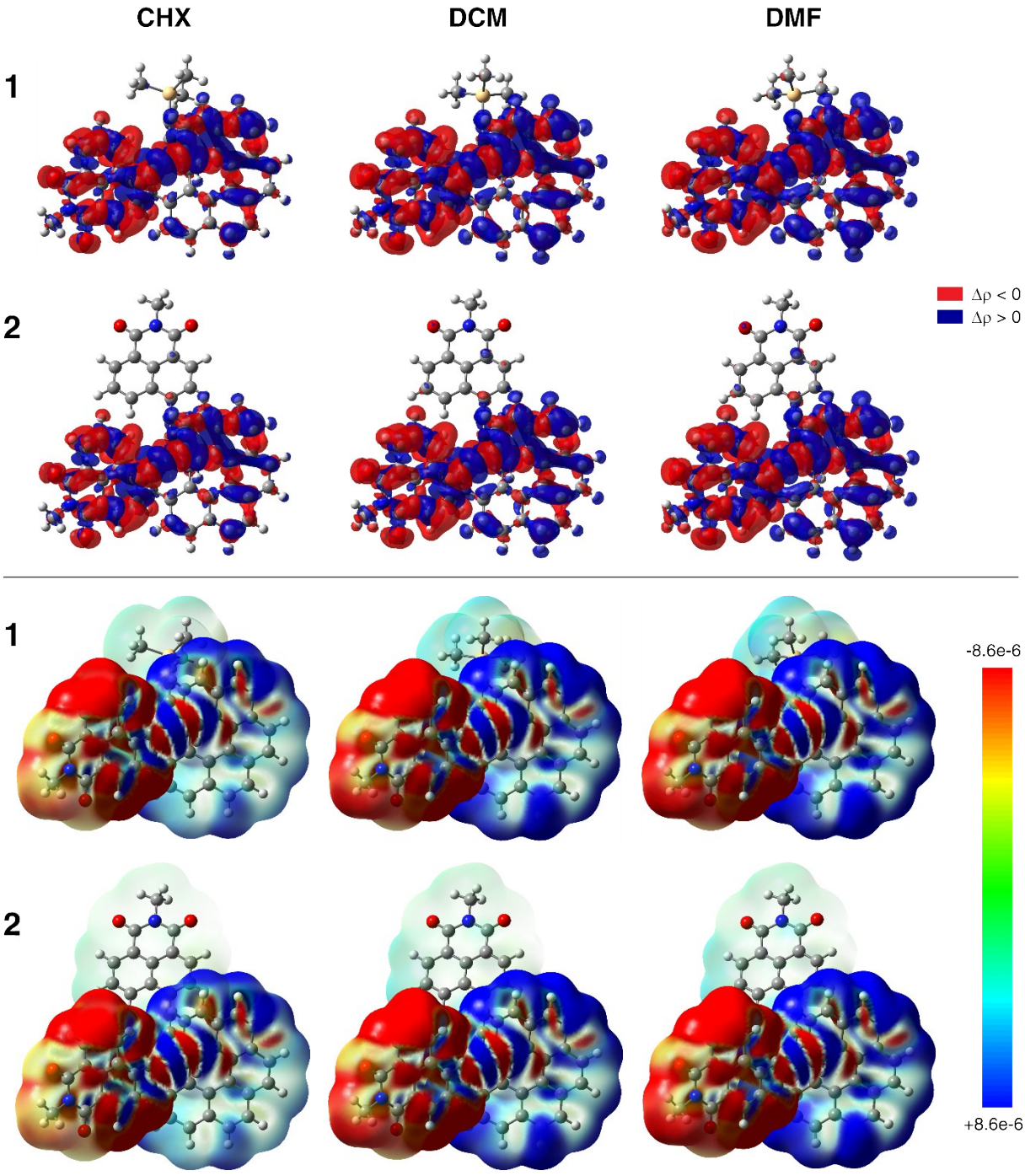

Figure S32. Isosurfaces (±0.0003 au) of the difference density between the S_0 ground state and S_1 excited state, $\Delta\rho = \rho_g - \rho_e$ (top) along with isosurfaces (0.0003 au) of ρ_g color-mapped using the value of $\Delta\rho$ (bottom) for the helicene-naphthalimide derivatives **1** (conformer I) and **2** (conformer I) based on the TDDFT BHLYP/SV(P) SS-PCM solvent calculations at S_1 TDDFT BHLYP/SV(P) LR-PCM solvent optimized geometries. Electron density moves from the red region to the blue region when moving from the excited state to the ground state. The corresponding isosurfaces for conformers II and III of **1** and **2** appeared to be very similar and therefore they are not shown. CHX, DCM, and DMF stand for cyclohexane, dichloromethane, and dimethylformamide solvent, respectively.

Table S15. Characteristics of $S_1 \rightarrow S_0$ transitions for helicene-naphthalimide derivatives **1** and **2** based on the TDDFT BHLYP/SV(P) calculations with continuum solvent model.[a]

	1		**2**		
	I	**II**	**I**	**II**	**III**
CHX					
d / au	3.773	3.554	3.834	3.651	3.726
m / au	2.130	3.022	2.336	2.758	2.561
θ / deg	74.75	78.17	66.04	68.19	67.04
R / 10^{-40} cgs	498.40	519.07	857.23	881.69	877.65
H-L / %	84.2	85.6	81.2	83.0	83.1
DCM					
d / au	3.776	3.569	3.833	3.651	3.714
m / au	1.891	2.785	2.125	2.573	2.388
θ / deg	74.70	78.25	68.80	70.69	69.79
R / 10^{-40} cgs	444.13	477.19	694.35	732.13	722.01
H-L / %	82.8	84.5	78.4	80.9	80.4
DMF					
d / au	3.734	3.534	3.794	3.614	3.665
m / au	1.803	2.704	2.021	2.485	2.318
θ / deg	74.74	78.32	69.33	71.30	70.65
R / 10^{-40} cgs	417.83	456.12	637.86	678.63	663.66
H-L / %	83.5	85.3	78.8	81.3	80.9

[a] *d* – electric transition dipole moment value. *m* – magnetic transition dipole moment value. θ – angle between vectors d and m. *R* – rotatory strength. H-L – percentage contribution of LUMO→HOMO transition to the $S_1 \rightarrow S_0$ emission. TDDFT BHLYP/SV(P) SS-PCM solvent calculations at S_1 TDDFT BHLYP/SV(P) LR-PCM solvent optimized geometries. CHX, DCM, and DMF stand for cyclohexane, dichloromethane, and dimethylformamide solvent, respectively. Compare with Figure S33.

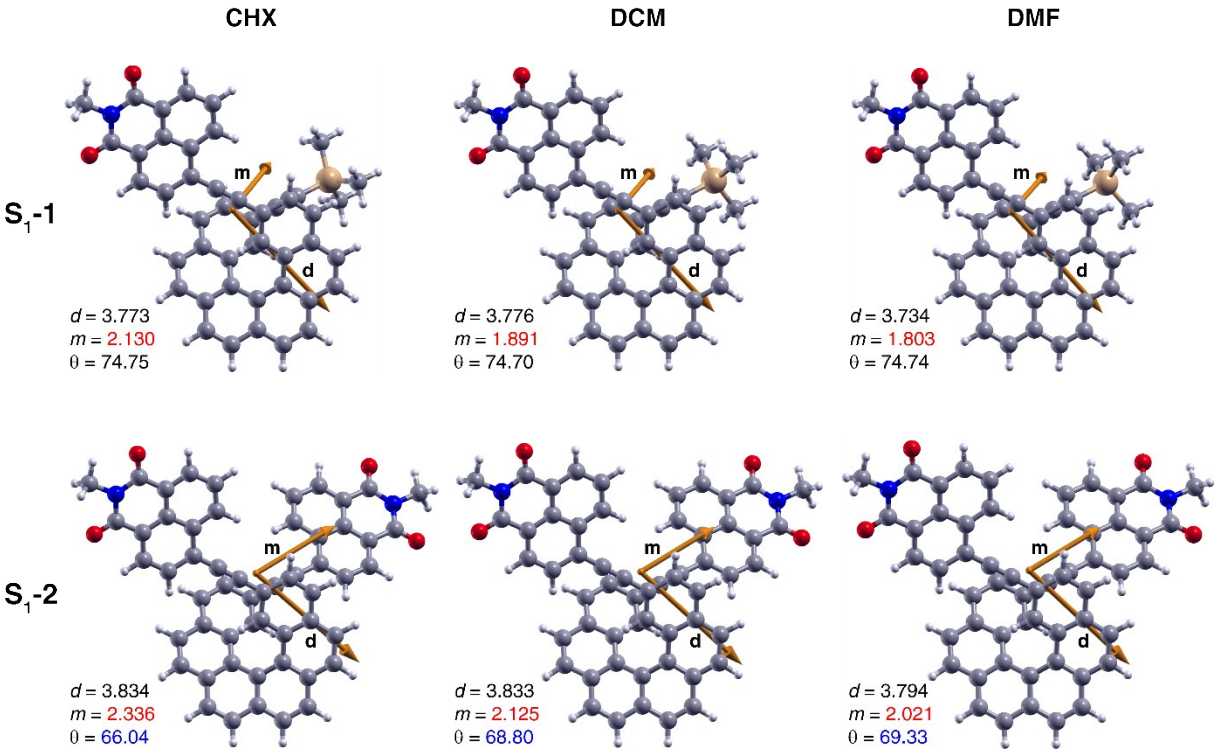

Figure S33. Electric (d) and magnetic (m) transition dipole moment vectors (orange vectors with origin located at the center of nuclear charge, scaled by a factor of 2) in the S_1 excited state for the helicene-naphthalimide derivatives **1** (conformer I) and **2** (conformer I) based on the TDDFT BHLYP/SV(P) SS-PCM solvent calculations at S_1 TDDFT BHLYP/SV(P) LR-PCM solvent optimized geometries. Numbers listed are corresponding electric *d* and magnetic *m* transition dipole moment values, in au, and angle θ between vectors d and m, in deg (those of them which change the most with a change of solvent polarity are highlighted in color). Transition dipole moments for conformers II and III of S_1-**1** and S_1-**2** appeared to be very similar and therefore they are not shown. CHX, DCM, and DMF stand for cyclohexane, dichloromethane, and dimethylformamide solvent, respectively. Compare with Table S15.

Optimized (BP/SV(P) with dichloromethane continuum solvent model) geometries of NPhBr and helicene-naphthalimide model systems along with their corresponding absolute energies

The atomic symbol followed by three Cartesian coordinates, in Å.

NPhBr

Total energy = -3279.126977 au

C	0.4976715	0.0032902	-1.1404762
C	0.5017826	0.0042324	0.2859377
C	1.7596048	0.0022979	0.9940518
C	2.9665969	0.0010684	0.2346351
C	2.9358365	0.0013093	-1.1572916
C	1.7009831	0.0015068	-1.8489530
C	-0.7314742	0.0035843	1.0001158
C	1.7021176	0.0012516	2.4272743
H	3.9309538	-0.0006348	0.7660370
H	3.8797059	-0.0000033	-1.7252620
H	1.6680255	-0.0000848	-2.9495663
C	0.4899202	0.0013230	3.1144833
C	-0.7276743	0.0015892	2.3961353
H	0.4772543	0.0000700	4.2148278
H	-1.6884778	-0.0002313	2.9341752
Br	3.3130036	-0.0012648	3.4512815
C	-0.7871154	-0.0028619	-1.8930656
C	-2.0300478	-0.0017333	0.2768367
N	-1.9724300	0.0131354	-1.1313943
O	-3.1163005	-0.0184188	0.8591258
O	-0.8352387	-0.0211436	-3.1244189
C	-3.2456038	0.0068695	-1.8600068
H	-3.5801568	-1.0363541	-2.0539543
H	-4.0074235	0.5185720	-1.2427388
H	-3.1015133	0.5226306	-2.8277897

***P*-1-I**

Total energy = -2264.893541 au

C	-1.3937472	-4.5256650	7.1960440
C	-1.0746194	-3.3255241	6.3756000
C	-0.4071216	-3.4578467	5.1214279
C	-0.0359455	-4.7485813	4.6437052
C	-0.3360519	-5.9626653	5.4406373
N	-0.9998997	-5.7736619	6.6687737
C	0.6150577	-4.8732346	3.4110267
C	0.9069845	-3.7379691	2.6316258
C	0.5577115	-2.4419529	3.0679291
C	-0.1140659	-2.2840968	4.3440089
C	-1.4391689	-2.0611322	6.8468974
C	-1.1499610	-0.9042388	6.0855440
C	-0.5005573	-1.0137466	4.8570023
C	0.8585282	-1.3130857	2.2611635
C	1.1176733	-0.3414486	1.5435149
C	1.4109766	0.7886504	0.7292134
C	1.2541569	2.1145332	1.2497528
C	1.6186871	3.2011532	0.4729644
C	2.1231711	3.0363491	-0.8514293
C	2.1914761	1.7154526	-1.4302200
C	1.8673104	0.6163255	-0.5933775
C	2.6820224	1.5530989	-2.8006504
C	3.3723816	2.6692912	-3.3811632
C	3.2819639	3.9707722	-2.7771858
C	2.6263080	4.1618132	-1.5818987
C	2.6241730	0.3087667	-3.5592218
C	3.6447366	0.1072897	-4.5582242
C	4.4093043	1.2185898	-5.0392528
C	4.1999422	2.4840803	-4.5356445
C	1.6335853	-0.7512965	-3.4017083
C	1.9844729	-2.0728567	-3.8378030
C	3.1536412	-2.2814353	-4.6389889
C	3.8975664	-1.2054015	-5.0716383
C	0.2578672	-0.5449637	-2.9427472
C	-0.5706393	-1.6899090	-2.6500648
C	-0.0752249	-3.0127537	-2.8961115
C	1.1365286	-3.1904924	-3.5232774
C	-1.9039038	-1.4934761	-2.1840011
C	-2.4512971	-0.2257542	-2.0668912
C	-1.6765606	0.9188076	-2.4405359
C	-0.3453674	0.7386440	-2.8610790
C	-2.2532937	2.2264464	-2.3929087
C	-2.7633277	3.3534104	-2.3429934
Si	-3.5057755	5.0528214	-2.2318856
O	-0.0344481	-7.1021126	5.0753235
C	-1.2944464	-6.9856148	7.4399154
O	-1.9727464	-4.4496874	8.2821865
H	0.8764987	2.2557023	2.2744898
H	1.5486521	4.2212105	0.8858965
H	2.5445085	5.1674992	-1.1375432
H	3.7600080	4.8191546	-3.2947519
H	4.7273006	3.3554964	-4.9575434
H	5.1428474	1.0445554	-5.8440755
H	4.7218057	-1.3405521	-5.7915343
H	3.3954456	-3.3053233	-4.9688164
H	1.4792096	-4.1998033	-3.8064311
H	-0.7115293	-3.8764725	-2.6413780
H	-2.5121450	-2.3808855	-1.9413722
H	-3.4867740	-0.0899637	-1.7172931
H	0.2233422	1.6266888	-3.1668319
H	2.0035746	-0.4083239	-0.9637266
H	1.4179531	-3.8569841	1.6638972
H	0.8950443	-5.8783110	3.0585638
H	-0.3530298	-7.5239756	7.6763116
H	-1.9464376	-7.6629074	6.8494926

H	-1.8047693	-6.6760445	8.3701482
H	-0.2786956	-0.1113186	4.2651509
H	-1.4415828	0.0875828	6.4668479
H	-1.9535550	-1.9855328	7.8175338
C	-2.9356625	5.8394268	-0.6016716
C	-2.8977689	6.0713749	-3.7123604
C	-5.3950752	4.8868331	-2.2667514
H	-3.3722711	6.8582381	-0.4909604
H	-3.2564464	5.2287735	0.2716493
H	-1.8272873	5.9323112	-0.5688921
H	-3.3239622	7.0997714	-3.6721952
H	-1.7881717	6.1578409	-3.7135862
H	-3.2090366	5.6066506	-4.6745610
H	-5.8710598	5.8902064	-2.1794588
H	-5.7398755	4.4232642	-3.2180404
H	-5.7591124	4.2581249	-1.4235607

***P*-1-II**

Total energy = -2264.893317 au

C	-2.1320352	-1.1257694	-1.8545680
C	-0.7728889	-1.2786279	-2.2587831
C	0.0347976	-0.1069445	-2.4979591
C	-0.6090601	1.1571138	-2.4318482
C	-1.9632015	1.2948865	-2.0729614
C	-2.7212554	0.1245111	-1.7489366
C	-0.2269774	-2.5829371	-2.4976716
C	1.0179659	-2.7163241	-3.0690778
C	1.8475290	-1.5705721	-3.3274086
C	1.4364855	-0.2666808	-2.8915877
C	3.0604249	-1.7319001	-4.0728786
C	3.7915244	-0.6274316	-4.4539315
C	3.4738212	0.6698683	-3.9367213
C	2.4002549	0.8247311	-2.9865630
C	4.2235326	1.8127246	-4.3649056
C	3.9470715	3.0639519	-3.8572344
C	3.0578999	3.2061681	-2.7430056
C	2.3801704	2.0590836	-2.2106290
C	2.8885888	4.4951852	-2.1292862
C	2.1670788	4.6460448	-0.9663679
C	1.6726277	3.4931720	-0.2733956
C	1.8194975	2.1842039	-0.8638892
C	1.0991580	3.6189971	1.0272157
C	0.7454684	2.5077298	1.7740516
C	0.9809169	1.1962840	1.2458579
C	1.5004188	1.0615904	-0.0573607
C	0.7063055	0.0444498	2.0359655
C	0.4666977	-0.9425771	2.7395837
C	0.1766492	-2.0578958	3.5693989
C	0.5429679	-3.4033579	3.1696427
C	0.2266309	-4.4967646	4.0488779
C	-0.4366079	-4.2558539	5.2873873
C	-0.7792997	-2.9482017	5.6497048
C	-0.4767600	-1.8634246	4.8054660
C	1.2074847	-3.6871802	1.9433043
C	1.5468284	-4.9943730	1.5978374
C	1.2341486	-6.0678634	2.4647712
C	0.5815770	-5.8279206	3.6771748
C	-0.7656811	-5.3787691	6.1983469
N	-0.3920739	-6.6715238	5.7808279
C	0.2657319	-6.9759236	4.5703968
O	-1.3389986	-5.2249219	7.2800812
C	-0.7234618	-7.7693363	6.6947534
O	0.5577457	-8.1386686	4.2813169
C	-2.5688910	2.5898918	-2.0420588
C	-3.0836234	3.7154202	-2.0143433
Si	-3.7946221	5.4306967	-1.9539299
H	0.3162255	2.6188366	2.7819469
H	0.9661150	4.6296679	1.4477481
H	2.0244573	5.6424713	-0.5166240
H	3.3584100	5.3675879	-2.6134328
H	4.4642064	3.9580314	-4.2431427
H	5.0006885	1.6742738	-5.1348809
H	4.6532826	-0.7272369	-5.1345762
H	3.3490057	-2.7432262	-4.4042460
H	1.4020769	-3.7111444	-3.3502112
H	-0.8483256	-3.4684415	-2.2841728
H	-2.7252698	-2.0330784	-1.6513538
H	-3.7756398	0.2252871	-1.4471322
H	-0.0533348	2.0647264	-2.7015203
H	1.6931865	0.0490577	-0.4361852
H	-0.7536889	-0.8420515	5.1086970
H	-1.2911275	-2.7809554	6.6102406
H	-1.8206383	-7.8098422	6.8586784
H	-0.2282401	-7.6100325	7.6753858
H	-0.3687780	-8.7088229	6.2330516
H	1.4528768	-2.8531473	1.2664720
H	2.0626265	-5.1954580	0.6453020
H	1.4983551	-7.1039158	2.2012365
C	-3.9458971	5.9464519	-0.1339082
C	-2.6114497	6.5895833	-2.8791741
C	-5.4971217	5.4135378	-2.7895654
H	-5.9421240	6.4346066	-2.7756270
H	-5.4187282	5.0865597	-3.8505524
H	-6.1974202	4.7250422	-2.2659037
H	-2.9952734	7.6350232	-2.8526045
H	-1.5991860	6.5807021	-2.4169615
H	-2.5071385	6.2869830	-3.9451534
H	-4.3512946	6.9812906	-0.0582854
H	-4.6295233	5.2662830	0.4217574
H	-2.9538757	5.9263879	0.3700372

***P*-2-I**

Total energy = -2560.784357 au

C	-6.0563738	4.6405801	-0.1116057
C	-5.3306038	5.6398967	-0.7658512
C	-4.1141691	5.3184681	-1.4387433
C	-3.6391373	3.9609173	-1.4411195
C	-4.4058925	2.9704589	-0.7645521

C	-5.5917567	3.3041234	-0.1122209
C	-2.3978705	3.6582381	-2.1271054
C	-1.6952789	4.7011723	-2.7682612
C	-2.1798012	6.0225264	-2.7564477
C	-3.3753660	6.3409490	-2.1024568
C	-5.8429338	7.0371441	-0.7489456
N	-5.0690209	8.0015247	-1.4287601
C	-3.8609767	7.7421885	-2.1058093
C	-1.8825301	2.3353194	-2.1614901
C	-1.4001399	1.1990145	-2.2113478
C	-0.8349520	-0.1059234	-2.2773756
C	0.4828158	-0.2799412	-2.7466498
C	1.0833205	-1.5603536	-2.8576270
C	0.2635307	-2.7095448	-2.5562026
C	-1.0524397	-2.5194943	-2.0378744
C	-1.5952294	-1.2545786	-1.8831221
C	0.7495585	-4.0263930	-2.8459566
C	1.9400891	-4.1899719	-3.5179545
C	2.7820912	-3.0678482	-3.8324956
C	2.4462854	-1.7570438	-3.3557379
C	3.9296159	-3.2578267	-4.6688025
C	4.6655581	-2.1714608	-5.0902525
C	4.4298697	-0.8721649	-4.5357369
C	3.4331842	-0.6943691	-3.5087350
C	5.1859613	0.2502828	-5.0041779
C	4.9894685	1.5025567	-4.4635363
C	4.1856053	1.6605393	-3.2883033
C	3.5060038	0.5311163	-2.7212166
C	4.1076810	2.9474654	-2.6524389
C	3.4706047	3.1111959	-1.4430916
C	2.9758059	1.9697735	-0.7316577
C	3.0372912	0.6617329	-1.3396747
C	2.4845856	2.1052952	0.6012049
C	2.1276847	1.0015286	1.3570835
C	2.2805568	-0.3130335	0.8070794
C	2.7246599	-0.4559969	-0.5228868
C	1.9902399	-1.4578876	1.6020165
C	1.7268573	-2.4349077	2.3106943
C	1.4197120	-3.5586540	3.1228508
C	0.7282907	-3.3875236	4.3869663
C	0.4402089	-4.5511950	5.1810090
C	0.8319436	-5.8452484	4.7294960
C	1.4941038	-5.9836541	3.5042909
C	1.7831372	-4.8581747	2.7093834
C	0.3171730	-2.1140054	4.8725120
C	-0.3507976	-1.9922142	6.0898171
C	-0.6318540	-3.1389704	6.8692822
C	-0.2426599	-4.4058424	6.4254672
C	0.5445023	-7.0485652	5.5475409
N	-0.1329508	-6.8462139	6.7663853
C	-0.5501839	-5.5945197	7.2664172
O	0.8689738	-8.1892603	5.2074195
C	-0.4112684	-8.0464621	7.5615153
O	-1.1379685	-5.5061614	8.3469107
O	-6.8883322	7.3513117	-0.1752894
C	-5.5353832	9.3916700	-1.4428447
O	-3.2605204	8.6632477	-2.6654731
H	1.7590890	1.1201901	2.3879507
H	2.4169724	3.1161613	1.0366353
H	3.3965447	4.1064343	-0.9745082
H	4.5787015	3.8069879	-3.1580382
H	5.5091236	2.3839715	-4.8742545
H	5.9012439	0.0966994	-5.8291907
H	5.4709253	-2.2885837	-5.8342395
H	4.1606060	-4.2729135	-5.0319270
H	2.2706625	-5.1932075	-3.8350770
H	0.1228426	-4.8962557	-2.5888920
H	-1.6510845	-3.4103770	-1.7848684
H	-2.6168890	-1.1241523	-1.4935068
H	1.0398291	0.6110796	-3.0650914
H	2.8578879	-1.4720000	-0.9172378
H	-0.7530174	4.4704129	-3.2885327
H	-1.6227625	6.8256688	-3.2638135
H	-5.6688759	9.7358233	-2.4894784
H	-4.7894679	10.0492864	-0.9489582
H	-6.4969779	9.4285187	-0.8992735
H	-4.0462988	1.9289203	-0.7618649
H	-6.1718327	2.5246371	0.4071435
H	-6.9914665	4.9148301	0.4011083
H	2.3055756	-4.9887116	1.7492442
H	1.7871445	-6.9918642	3.1718702
H	0.5397317	-8.5385966	7.8552465
H	-1.0094482	-8.7657632	6.9646180
H	-0.9716518	-7.7311679	8.4604821
H	0.5338680	-1.2187504	4.2680312
H	-0.6628693	-0.9983469	6.4485274
H	-1.1586849	-3.0537638	7.8323831

***P*-2-II**

Total energy = -2560.784324 au

C	2.2208184	-7.1519300	2.6364235
C	1.5592276	-6.9225617	3.8459448
C	1.1963193	-5.5954466	4.2240025
C	1.5114667	-4.4957346	3.3525135
C	2.1851669	-4.7686805	2.1286876
C	2.5341112	-6.0718120	1.7779762
C	0.5263981	-5.3645714	5.4608499
C	0.1944571	-6.4951127	6.3615770
N	0.5732837	-7.7838785	5.9366136
C	1.2413385	-8.0776197	4.7291907
C	1.1344309	-3.1549355	3.7571926
C	0.4780717	-2.9695917	4.9929082
C	0.1783534	-4.0604600	5.8305556
C	1.4161575	-2.0359955	2.9293417
C	1.6484215	-1.0496076	2.2225931
C	1.9181921	0.1032873	1.4322278
C	2.4251809	-0.0283077	0.1235462

C	2.7484692	1.0968267	-0.6781925
C	2.6143153	2.4035312	-0.0795746
C	2.0491763	2.5265240	1.2248882
C	1.6944681	1.4135039	1.9686384
C	3.3043737	0.9762978	-2.0274003
C	3.9919396	2.1205035	-2.5530400
C	3.8346818	3.4073166	-1.9316274
C	3.1157683	3.5569476	-0.7669493
C	3.3108989	-0.2517576	-2.8132958
C	4.3808769	-0.4102922	-3.7671049
C	5.1439220	0.7273573	-4.1852450
C	4.8801215	1.9771916	-3.6677978
C	2.3333186	-1.3311081	-2.7297195
C	2.7239091	-2.6342301	-3.1861091
C	3.9339740	-2.8039738	-3.9341024
C	4.6805742	-1.7051634	-4.3005146
C	0.9335458	-1.1571615	-2.3337332
C	0.1056790	-2.3201753	-2.1178172
C	0.6310891	-3.6278761	-2.3774109
C	1.8759648	-3.7702932	-2.9475644
C	0.3084897	0.1138846	-2.2502983
C	-1.0484094	0.2642784	-1.8984848
C	-1.8273152	-0.8997287	-1.5968934
C	-1.2541235	-2.1546750	-1.7175941
C	-1.6324746	1.5618427	-1.8577025
C	-2.1286492	2.6927819	-1.8254675
C	-2.6482522	4.0138605	-1.7899372
C	-1.7780342	5.1126313	-1.9570263
C	-2.2572272	6.4353739	-1.9211091
C	-3.6168387	6.6988574	-1.7197323
C	-4.5309238	5.6181446	-1.5515413
C	-4.0624411	4.2587790	-1.5835881
C	-5.9187826	5.8822960	-1.3518826
C	-6.4277428	7.2804728	-1.3126448
N	-5.4726650	8.3050340	-1.4835529
C	-4.0929913	8.1027769	-1.6830897
C	-5.0081213	3.2083496	-1.4145978
C	-6.3604606	3.4863376	-1.2226126
C	-6.8183099	4.8248086	-1.1908100
O	-3.3432003	9.0734158	-1.8175215
C	-5.9256606	9.6992780	-1.4518113
O	-7.6195199	7.5458449	-1.1402981
O	-0.3865851	-6.3504871	7.4403103
C	0.2364202	-8.8896369	6.8388339
O	1.5394604	-9.2372471	4.4340242
H	1.2747149	1.5220529	2.9808037
H	1.9260341	3.5359510	1.6514200
H	2.9828043	4.5513813	-0.3098803
H	4.3128153	4.2783185	-2.4100234
H	5.4068139	2.8689223	-4.0458968
H	5.9199300	0.5872453	-4.9559530
H	5.5399013	-1.8081954	-4.9837446
H	4.2072460	-3.8145225	-4.2800946
H	2.2447591	-4.7663149	-3.2443731
H	-0.0045327	-4.5073926	-2.1829038
H	-1.8600767	-3.0569043	-1.5314684
H	-2.8816981	-0.7879918	-1.2995563
H	0.8771606	1.0177542	-2.5047625
H	2.6078753	-1.0402518	-0.2624033
H	-0.7051532	4.9246556	-2.1158909
H	-1.5658500	7.2826787	-2.0505723
H	-5.6447216	10.2098941	-2.3961623
H	-5.4468482	10.2372899	-0.6066856
H	-7.0239158	9.6930573	-1.3276049
H	-4.6546068	2.1650006	-1.4392904
H	-7.0787184	2.6606206	-1.0951263
H	-7.8846267	5.0548035	-1.0404366
H	0.1948291	-1.9513243	5.3006985
H	-0.3368568	-3.9006258	6.7906065
H	-0.8604138	-8.9227108	7.0055803
H	0.7360061	-8.7464592	7.8198334
H	0.5824678	-9.8263878	6.3653308
H	2.4307180	-3.9291206	1.4587763
H	3.0579821	-6.2647004	0.8280793
H	2.4918576	-8.1850076	2.3682560

***P*-2-III**

Total energy = -2560.784127 au

C	-0.5809436	7.6904049	-2.4431437
C	-1.9210759	7.7644138	-2.0537283
C	-2.6506635	6.5726767	-1.7653106
C	-2.0004277	5.2950202	-1.8786696
C	-0.6349374	5.2595224	-2.2791802
C	0.0615818	6.4348574	-2.5553502
C	-2.7622553	4.0959442	-1.5860749
C	-4.1128899	4.2189183	-1.1950793
C	-4.7288625	5.4802786	-1.0867170
C	-4.0172558	6.6519303	-1.3679771
C	-2.5725071	9.0983035	-1.9468879
N	-3.9272419	9.1093847	-1.5529861
C	-4.6942095	7.9664610	-1.2517274
C	-2.1668703	2.8110715	-1.6950325
C	-1.6625537	1.6872418	-1.7917325
C	-1.1140195	0.3785077	-1.9081602
C	0.2741625	0.1924295	-2.0663217
C	0.8532759	-1.0947994	-2.2152805
C	-0.0439214	-2.2236221	-2.2876188
C	-1.4421728	-2.0281678	-2.0806600
C	-1.9758258	-0.7662247	-1.8806356
C	0.4638396	-3.5174883	-2.6365159
C	1.7784406	-3.6627375	-3.0181382
C	2.6996348	-2.5608029	-2.9605176
C	2.2912392	-1.3046670	-2.3996649
C	4.0115114	-2.7105147	-3.5161271
C	4.8563059	-1.6249521	-3.5971924
C	4.5252474	-0.3944340	-2.9438011
C	3.3136514	-0.2906316	-2.1682137

C	5.4009689	0.7324855	-3.0624384
C	5.1110680	1.9160449	-2.4188518
C	4.0506508	1.9701739	-1.4571626
C	3.2258581	0.8189190	-1.2260308
C	3.8543542	3.1682531	-0.6875002
C	2.9486920	3.2132157	0.3483001
C	2.2706621	2.0202880	0.7616483
C	2.4446291	0.7985656	0.0126094
C	1.4823235	2.0118423	1.9509464
C	0.9407809	0.8404846	2.4525507
C	1.1955960	-0.4008878	1.7827422
C	1.9269300	-0.3959839	0.5777804
C	0.7300816	-1.6218765	2.3482249
C	0.3236205	-2.6627089	2.8754959
C	-0.1537217	-3.8422971	3.5064951
C	0.2239132	-5.1552559	3.0195234
C	-0.2824159	-6.3170304	3.6993816
C	-1.1414365	-6.1734228	4.8276435
C	-1.4911896	-4.8953083	5.2774383
C	-1.0042969	-3.7447817	4.6288523
C	1.0806458	-5.3425131	1.8983185
C	1.4249876	-6.6220067	1.4654826
C	0.9254650	-7.7630634	2.1366068
C	0.0810557	-7.6183041	3.2407025
C	-1.6679688	-7.3674698	5.5323069
N	-1.2756800	-8.6268567	5.0370813
C	-0.4287654	-8.8359855	3.9281995
O	-2.4164639	-7.2980800	6.5106976
C	-1.8028202	-9.7964043	5.7473009
O	-0.1346804	-9.9753246	3.5592402
O	-1.9723944	10.1482464	-2.1881358
C	-4.6132512	10.4002728	-1.4386839
O	-5.8735723	8.0904074	-0.9111246
H	0.3467423	0.8453784	3.3795619
H	1.3339964	2.9621040	2.4901885
H	2.7897591	4.1428805	0.9191069
H	4.4564988	4.0559200	-0.9437162
H	5.7372781	2.8106748	-2.5704243
H	6.2911461	0.6427789	-3.7069542
H	5.8162107	-1.6945220	-4.1353267
H	4.2973936	-3.6834574	-3.9486854
H	2.1508048	-4.6335990	-3.3854764
H	-0.2299690	-4.3737294	-2.6648302
H	-2.1060680	-2.9080119	-2.1108607
H	-3.0585722	-0.6276813	-1.7364318
H	0.9142867	1.0837116	-2.1074150
H	2.1285035	-1.3588785	0.0897973
H	-4.6901571	3.3089453	-0.9702774
H	-5.7832893	5.5616671	-0.7796607
H	-4.9681454	10.5524397	-0.3978645
H	-5.4923487	10.4240011	-2.1159437
H	-3.8912346	11.1894409	-1.7171278
H	-0.1327628	4.2828364	-2.3684839
H	1.1181597	6.3888436	-2.8642384
H	-0.0402848	8.6249022	-2.6599083
H	-1.2895217	-2.7481004	4.9990090
H	-2.1553457	-4.8044515	6.1511186
H	-2.9123700	-9.7948820	5.7121509
H	-1.4858038	-9.7696124	6.8107206
H	-1.4040085	-10.6991060	5.2495413
H	1.4720597	-4.4554817	1.3747110
H	2.0910893	-6.7487199	0.5970391
H	1.1920707	-8.7782530	1.8034843